Journal of Mathematical Biology (2023) 86:52
https://doi.org/10.1007/s00285-023-01887-8

Mathematical Biology

Relative prevalence-based dispersal in an epidemic patch model

Min Lu[1] · Daozhou Gao[2,3] · Jicai Huang[1] · Hao Wang[4]

Received: 28 September 2022 / Revised: 21 January 2023 / Accepted: 11 February 2023

Abstract

In this paper, we propose a two-patch SIRS model with a nonlinear incidence rate: $\beta_i(1+\nu_i I_i)I_i S_i$ and nonconstant dispersal rates, where the dispersal rates of susceptible and recovered individuals depend on the relative disease prevalence in two patches. In an isolated environment, the model admits Bogdanov–Takens bifurcation of codimension 3 (cusp case) and Hopf bifurcation of codimension up to 2 as the parameters vary, and exhibits rich dynamics such as multiple coexistent steady states and periodic orbits, homoclinic orbits and multitype bistability. The long-term dynamics can be classified in terms of the infection rates β_i (due to single contact) and ν_i (due to double exposures). In a connected environment, we establish a threshold $R_0 = 1$ between disease extinction and uniform persistence under certain conditions. We numerically explore the effect of population dispersal on disease spread when $\nu_i = 0$ and patch 1 has a lower infection rate, our results indicate: **(i)** R_0 can be nonmonotonic in dispersal rates and $R_0 \leq \max\{R_{01}, R_{02}\}$ (R_{0i} is the basic reproduction number of patch i) may fail; **(ii)** the constant dispersal of susceptible individuals (or infective individuals) between two patches (or from patch 2 to patch 1) will increase (or reduce) the overall disease prevalence; **(iii)** the relative prevalence-based dispersal may reduce the overall disease prevalence. When $\nu_i > 0$ and the disease outbreaks periodically in each isolated patch, we find that: **(a)** small unidirectional and constant dispersal can lead to complex periodic patterns like relaxation oscillations or mixed-mode oscillations, whereas large ones can make the disease go extinct in one patch and persist in the

In memory of Fred G. Brauer (1932–2021).

Research was partially supported by NSFC (Nos. 11871235, 12231008 and 12071300) and NSERC (RGPIN-2020-03911 and RGPAS-2020-00090).

✉ Jicai Huang
hjc@mail.ccnu.edu.cn

✉ Hao Wang
hao8@ualberta.ca

Extended author information available on the last page of the article

Published online: 06 March 2023

form of a positive steady state or a periodic solution in the other patch; **(b)** relative prevalence-based and unidirectional dispersal can make periodic outbreak earlier.

Keywords SIRS patch model · Nonlinear incidence rate · Nonconstant dispersal · Bogdanov–Takens bifurcation · Hopf bifurcation · Disease prevalence · Mixed-mode oscillations

Mathematics Subject Classification 92D30 · 34C23

1 Introduction

Infectious diseases pose a serious threat to global public health and economic growth. Over the past few decades, globalization, urbanization and the development of rapid transit networks have pushed migration and tourism to an unprecedented level until the emergence of COVID-19. For example, the degree of urbanization, i.e., the percentage of total population lives in cities, in the world increased from 47% of 6.11 billion people in 2000 to 56.2% of 7.75 billion people in 2020 (The World Bank Group 2022b). Meanwhile, the total number of air passengers increased from 1.67 billion in 2000 to 4.56 billion in 2019, but dropped dramatically to 1.81 billion in 2020 (The World Bank Group 2022a). Massive population movement is a key factor for the introduction, transmission and spread of infectious diseases. On the one hand, increasing human mobility makes emerging and re-emerging pathogens easily spread from one location to another. The first Zika virus infection in Brazil was reported in May 2015 and the disease spread to more than 60 countries in the Americas, the Pacific Islands, South-east Asia and Africa by April 2016. On the other hand, persistent imported cases constitute a major challenge for achieving and maintaining disease elimination status in low transmission regions. This is the reason why many countries have lifted travel restrictions and chosen to live alongside COVID-19. There is an urgent need for policy makers to understand the impact of population dispersal on the spread of infectious diseases.

Many mathematical models with the consideration of population movement and spatial heterogeneity have been developed and analyzed in recent years. When host movement in a discrete space is considered, multi-patch epidemic models in the form of ordinary differential equations are widely adopted. For instance, Wang and Mulone (2003) formulated a two-patch SIS model and showed that population dispersal can lead to disease persistence in both patches even if the disease disappears in one patch and persists in the other patch in isolation. Later on, Wang and Zhao (2004) and Jin and Wang (2005) investigated a similar SIS model except that the incidence rate is bilinear and the number of patches is arbitrary. They found that a disease can spread/die out in all patches, even though it is extinct/persistent in each isolated patch. Based on a multi-patch SIS model, Allen et al. (2007) discovered that the endemic equilibrium converges to a spatially inhomogeneous disease-free equilibrium as the diffusion rate of the susceptible population approaches zero. van den Driessche and coauthors extended the SIS patch model by incorporating latency and acquired immunity (Salmani and van den Driessche 2006; Hsieh et al. 2007). Cosner et al. (2009) constructed two classes of epidemic patch models for vector-borne diseases using Lagrangian and Eulerian

approaches, respectively. Arino et al. (2012) built a multi-patch malaria model with SIRS and SI structures for hosts and vectors, respectively, and identified infection reservoirs for disease eradication. Gao et al. (2013) developed a three-patch epidemic model to describe the spatial spread of Rift Valley fever in Egypt. Recently (Zhang et al. 2023a) formulated and analyzed multi-patch models under memory-based dispersal, and Zhang et al. (2023b) studied perceptive movement of susceptible individuals with memory, following the recent PDE guidance for cognitive movement (Wang and Salmaniw 2022). These theoretical studies mainly focus on establishing threshold dynamic results in terms of the basic reproduction number R_0 and bifurcations (Wang and Mulone 2003; Wang and Zhao 2004; Jin and Wang 2005; Salmani and van den Driessche 2006; Hsieh et al. 2007; Gao et al. 2013; Zhang et al. 2023b, a), analyzing the dependence of R_0 on model parameters especially the travel-related parameters (Allen et al. 2007; Gao and Ruan 2012; Hsieh et al. 2007), and exploring the impact of population dispersal and cognitive memory on the endemic equilibrium (Allen et al. 2007; Gao 2020; Gao and Lou 2021; Zhang et al. 2023b, a). In addition, during the early phase of the COVID-19 pandemic, metapopulation models have been extensively used to simulate the epidemics across different areas (Chinazzi et al. 2020; Wu et al. 2020). During the late phase of the COVID-19 pandemic, metapopulation models have been applied with sufficient data to explore infectivity and fatality of SARS-CoV-2 mutations (Xue et al. 2022).

The standard/bilinear incidence rate is a good approximation for a large/small population. There are few exceptions but under which the disease dynamics are not fully understood (Arino et al. 2012; Hsieh et al. 2007). In recent years, researchers have proposed quite a few novel incidence rates such as saturated incidence rate and non-monotone incidence rate. The interested reader may refer to the introduction of a recent paper by Lu et al. (2019, 2021) and Pan et al. (2022) for some details. The other factor is the changes in travel behavior caused by infections. During a serious disease outbreak, public health agencies issue travel alerts and advise citizens to avoid non-essential and non-urgent travel to high-risk countries or regions. In some extreme cases, strict border restrictions even border closure could be implemented to contain disease spread. Many people choose to work from home and shop online where possible, postpone or cancel business trips, change leisure and tourism destinations, and flee the epicenter. According to the International Organization for Migration (International Organization for Migration 2020), 219 countries, territories or areas had issued 98,717 travel restrictions in response to COVID-19 as of October 12, 2020. In the United States, the total number of domestic air passengers had year-over-year decreases of 51.0% in March 2020, 95.7% in April 2020 and 88.4% in May 2020 Hotle and Mumbower (2021).

Most spatial models assume that individuals from different disease states travel at different but constant rates (Wang and Mulone 2003; Salmani and van den Driessche 2006; Hsieh et al. 2007; Gao and Ruan 2012). In other words, they do address the infection-induced variation in mobility but disregard the change in travel behavior with the progression of an epidemic. Recently, Yang et al. (2020) developed an SIS patch model where the travel rate depends on the number of infectives of the destination patch but the incidence rate is standard, and Wang et al. (2022) formulated and compared different spatially heterogeneous diffusion operators for cognitive movement in SIS

epidemic models. This paper follows a similar idea of cognitive movement in Wang and Salmaniw (2022) to model the relative prevalence-based movement between patches.

To explore the joint effect of nontrivial incidence rate and infection-dependent dispersal on disease dynamics, we propose a two-patch SIRS model:

$$\begin{aligned}
\frac{dS_1}{dt} &= b_1 - d_1 S_1 - \lambda_1(I_1) I_1 S_1 + \gamma_1 R_1 - a_{12}\left(\frac{I_1}{N_1}, \frac{I_2}{N_2}\right) S_1 + a_{21}\left(\frac{I_2}{N_2}, \frac{I_1}{N_1}\right) S_2,\\
\frac{dI_1}{dt} &= \lambda_1(I_1) I_1 S_1 - (d_1 + \alpha_1) I_1 - b_{12} I_1 + b_{21} I_2,\\
\frac{dR_1}{dt} &= \alpha_1 I_1 - (d_1 + \gamma_1) R_1 - c_{12}\left(\frac{I_1}{N_1}, \frac{I_2}{N_2}\right) R_1 + c_{21}\left(\frac{I_2}{N_2}, \frac{I_1}{N_1}\right) R_2,\\
\frac{dS_2}{dt} &= b_2 - d_2 S_2 - \lambda_2(I_2) I_2 S_2 + \gamma_2 R_2 + a_{12}\left(\frac{I_1}{N_1}, \frac{I_2}{N_2}\right) S_1 - a_{21}\left(\frac{I_2}{N_2}, \frac{I_1}{N_1}\right) S_2,\\
\frac{dI_2}{dt} &= \lambda_2(I_2) I_2 S_2 - (d_2 + \alpha_2) I_2 + b_{12} I_1 - b_{21} I_2,\\
\frac{dR_2}{dt} &= \alpha_2 I_2 - (d_2 + \gamma_2) R_2 + c_{12}\left(\frac{I_1}{N_1}, \frac{I_2}{N_2}\right) R_1 - c_{21}\left(\frac{I_2}{N_2}, \frac{I_1}{N_1}\right) R_2,
\end{aligned} \tag{1.1}$$

where $S_i(t)$, $I_i(t)$ and $R_i(t)$ denote the number of susceptible, infectious and recovered individuals in patch i at time t, respectively, and $N_i = S_i(t) + I_i(t) + R_i(t)$ is the total population size of patch i at time t. In patch $i \in \{1, 2\}$, the parameter b_i represents the recruitment rate, d_i is the natural death rate, α_i is the recovery rate, γ_i is the rate of loss of immunity, and $\lambda_i(I_i)$ is the transmission rate. The rate at which susceptible, infectious and recovered individuals migrate from patch i to patch j for $i \neq j$ is denoted by $a_{ij}\left(\frac{I_1}{N_1}, \frac{I_2}{N_2}\right)$, b_{ij} and $c_{ij}\left(\frac{I_1}{N_1}, \frac{I_2}{N_2}\right)$, respectively. The ratio $\frac{I_i}{N_i}$ is called the disease prevalence of patch i, that is, the fraction of people being infected. Here the travel rates of infectives, b_{12} and b_{21}, are assumed to be constant, since infected people may no longer care about the epidemic or their travel is essential.

The nonlinear incidence rate we will adopted is of the form

$$\lambda_i(I_i) I_i S_i = \beta_i (1 + \nu_i I_i) I_i S_i \quad \text{with } \beta_i > 0 \text{ and } \nu_i \geq 0, \tag{1.2}$$

where $\beta_i I_i S_i$ represents the new infections caused by single contacts and $\beta_i \nu_i I_i^2 S_i$ is the new infective individuals arising from double exposures. The rate (1.2) was initially proposed by van den Driessche and Watmough (2000), later used by van den Driessche and Watmough (2003) and Jin et al. (2007) for SIRS model, Alexander and Moghadas (2004) for SIV model, Li et al. (2007, 2015) for SI model, and Li et al. (2014) for SIS model.

Furthermore, we assume that

$$a_{12}\left(\frac{I_1}{N_1}, \frac{I_2}{N_2}\right) = a_{12}(x) \text{ with } x = \theta_{12}^S \left(\frac{I_1}{N_1} - \frac{I_2}{N_2}\right),$$

where $\theta_{12}^S \in [0, 1]$ measures the degree to which the travel rate of the susceptible population from patch 1 to patch 2 depends on the relative severity of the epidemic on

the two patches, and the travel rate function $a_{12}(x)$ satisfies

$$\begin{aligned} &(A_1) \quad a_{12}(x) \text{ is an increasing function of } x;\\ &(A_2) \quad a_{12}(-1) = 0;\\ &(A_2) \quad a_{12}(0) = M_{12}^S \text{ with } M_{12}^S > 0. \end{aligned} \tag{1.3}$$

The first assumption (A_1) means that susceptible individuals of patch 1 leave more quickly as the relative disease severity of patch 1 to patch 2 becomes more serious. Assumption (A_2) guarantees the positivity of the travel rate. Indeed, $\frac{I_1}{N_1} - \frac{I_2}{N_2} = -1$ occurs if and only if no one in patch 1 is infected while everyone in patch 2 is infected. In this case, susceptible individuals do not move from patch 1 to patch 2. The last assumption (A_3) implies that the travel rate for susceptible individuals from patch 1 to patch 2 equals a constant M_{12}^S, the normal travel rate without considering the impact of travel behavior change, if the two patches have the same disease prevalence or the travel rate is independent of the relative severity, i.e., $\theta_{12}^S = 0$. The following three types of dispersal rate $a_{12}(x)$ with $x = \theta_{12}^S\left(\frac{I_1}{N_1} - \frac{I_2}{N_2}\right)$ satisfy the above assumptions:

$$\begin{aligned} &\text{Type I}: \ a_{12}(x) = k(1+x), \ \text{with } k = M_{12}^S;\\ &\text{Type II}: \ a_{12}(x) = \frac{k(1+x)}{a+(1+x)}, \ \text{with } k = M_{12}^S(a+1) \text{ and } a > 0;\\ &\text{Type III}: \ a_{12}(x) = \frac{k(1+x)^2}{1+a(1+x)+b(1+x)^2}, \ \text{with } k = M_{12}^S(1+a+b) \text{ and } a, b > 0. \end{aligned} \tag{1.4}$$

Similarly, $a_{21}\left(\frac{I_2}{N_2}, \frac{I_1}{N_1}\right) = a_{21}(x)\left(x = \theta_{21}^S\left(\frac{I_2}{N_2} - \frac{I_1}{N_1}\right)\right)$ has the same properties as $a_{12}(x)$ in (1.3) with $a_{21}(0) = M_{21}^S$. The travel rate $c_{ij}\left(\frac{I_i}{N_i}, \frac{I_j}{N_j}\right) = c_{ij}(x)\left(x = \theta_{ij}^R\left(\frac{I_i}{N_i} - \frac{I_j}{N_j}\right)\right)$ for $i \neq j$ has the same properties as $a_{ij}(x)$ with $c_{ij}(0) = M_{ij}^R$.

When two patches are disconnected, the disease dynamics of patch $i \in \{1, 2\}$ are described by

$$\begin{aligned} \frac{dS_i}{dt} &= b_i - d_i S_i - \lambda_i(I_i) I_i S_i + \gamma_i R_i,\\ \frac{dI_i}{dt} &= \lambda_i(I_i) I_i S_i - (d_i + \alpha_i) I_i,\\ \frac{dR_i}{dt} &= \alpha_i I_i - (d_i + \gamma_i) R_i. \end{aligned} \tag{1.5}$$

For system (1.5), it follows from the next generation matrix method (Diekmann et al. 2010; van den Driessche and Watmough 2002) that the basic reproduction number is $R_{0i} = \frac{b_i \beta_i}{d_i(d_i+\alpha_i)}$. When infections induced by double exposures are ignored, i.e., $\nu_i = 0$, the incidence rate is bilinear and the dynamic behavior of system (1.5) is clear. Namely, the disease-free equilibrium is globally asymptotically stable (i.e., the disease cannot invade the population) if $R_{0i} \leq 1$, whereas there exists a unique endemic equilibrium which is globally asymptotically stable (i.e., the disease can

invade a susceptible population) if $R_{0i} > 1$. However, R_{0i} may no longer serve as a sharp threshold quantity and the disease dynamics can be complex as $\nu_i > 0$. van den Driessche and Watmough (2003) showed the existence of saddle-node bifurcation, but they only focused on numerical examples to demonstrate the existence of Hopf bifurcation, homoclinic orbit and the attractive basin of an endemic equilibrium. Jin et al. (2007) theoretically obtained the existence of backward bifurcation, Hopf bifurcation and Bogdanov–Takens bifurcation. So far the complete bifurcation phenomena of system (1.5) is still unclear, especially for the high codimension bifurcations, such as degenerate Bogdanov–Takens bifurcation and Hopf bifurcations.

In this paper, for system (1.5) with $\nu_i > 0$, we will show that the codimension for degenerate Bogdanov–Takens bifurcation is up to 3 and the codimension for Hopf bifurcation is up to 2. The organizing center of bifurcation set is the cusp of codimension 3, originating from which there exist a series of bifurcations with lower codimension, such as codimension-1: saddle-node, Hopf, homoclinic bifurcations and bifurcation of a double limit cycle; codimension-2: Bogdanov–Takens bifurcation, degenerate Hopf bifurcation, degenerate homoclinic bifurcation, simultaneous occurrence of Hopf and homoclinic bifurcation. Moreover, (1.5) can exhibit rich dynamics such as multiple coexistent steady states or periodic orbits, homoclinic orbits and multitype bistability, etc. Our results indicate that we can classify the long-time dynamics of system (1.5) by the infection rates β_i (due to single contact) and ν_i (due to double exposures). More precisely, it is shown that there exists two critical values β^* and β_* with $\beta^* < \beta_*$ for β_i and two critical values $\frac{d_i}{b_i}$ and ν_* with $\frac{d_i}{b_i} < \nu_*$ for ν_i, which determine whether the disease dies out or persists in the form of coexistent positive periodic oscillations or coexistent steady states under different initial densities.

In a connected environment, we will first calculate the basic reproduction number R_0 for two-patch model (1.1), and then show the global asymptotic stability of the disease-free equilibrium if $R_0 < 1$ and $\nu_1 = \nu_2 = 0$, and the travel rates are independent of disease status and disease prevalence. Moreover, system (1.1) admits at least one endemic equilibrium and the disease is uniformly persistent if $R_0 > 1$ and the dispersal rates of infective individuals are positive. Therefore, we establish a threshold between extinction and uniform persistence of the disease for model (1.1) under certain conditions. By numerical simulations, we explored the effect of human migration on extinction, persistence and endemic level of infectious diseases. When the incidence rate is bilinear, i.e., $\nu_i = 0$ $(i = 1, 2)$, we will show that the relative prevalence-based dispersal for susceptible and recovered individuals may reduce the overall prevalence of the disease; when the incidence rate is nonlinear, i.e., $\nu_i > 0$ $(i = 1, 2)$, the relative prevalence-based and unidirectional dispersal for susceptible and recovered individuals can make periodic outbreak earlier.

The remaining parts of this paper is organized as follows. In Sect. 2, we study the global dynamics and bifurcations of the single-patch model (1.5) with $\nu_i > 0$. In Sect. 3, we investigate the dynamics of the two-patch model (1.1), we establish a threshold between extinction and uniform persistence of the disease in restricted conditions. Then, by numerical simulations, we analyze the effect of population dispersal on extinction, persistence and disease prevalence. A brief discussion is given in the last section.

2 Dynamics in isolated environment

We can clearly see that the total population of an isolated patch tends to a constant due to no disease-caused mortality.

Lemma 2.1 *The plane* $N_i := S_i + I_i + R_i = \frac{b_i}{d_i}$ *is an invariant manifold of system* (1.5)*, which is attracting in the first octant.*

The limit set of system (1.5) is contained in the plane $N_i = \frac{b_i}{d_i}$, on which system (1.5) can be reduced to the 2-dimensional system

$$\begin{aligned} \frac{dI_i}{dt} &= \beta_i(1+\nu_i I_i)I_i\left(\frac{b_i}{d_i} - I_i - R_i\right) - (d_i+\alpha_i)I_i, \\ \frac{dR_i}{dt} &= \alpha_i I_i - (d_i+\gamma_i)R_i. \end{aligned} \tag{2.1}$$

By letting $I = \beta_i I_i/(d_i+\gamma_i)$, $R = \beta_i R_i/(d_i+\gamma_i)$, and $\bar{t} = (d_i+\gamma_i)t$, system (2.1) can be rewritten as (still denote $\bar{t}$ by t)

$$\begin{aligned} \frac{dI}{dt} &= I(1+pI)(A-I-R) - \frac{A}{R_{0i}}I, \\ \frac{dR}{dt} &= qI - R, \end{aligned} \tag{2.2}$$

where

$$\begin{aligned} &p = \frac{\nu_i(d_i+\gamma_i)}{\beta_i} \geq 0, \quad A = \frac{b_i\beta_i}{d_i(d_i+\gamma_i)} > 0, \quad R_{0i} = \frac{b_i\beta_i}{d_i(d_i+\alpha_i)} > 0, \\ &q = \frac{\alpha_i}{d_i+\gamma_i} > 0. \end{aligned} \tag{2.3}$$

It is easy to verify that the inequality $qR_{0i} < A < (q+1)R_{0i}$ holds.

Denote

$$\begin{aligned} \Gamma &= \{(R_{0i}, p) \in \mathbb{R}^2 : \ R_{0i} > 0, \ p \geq 0\}, \\ \Lambda &= \{(A, q) \in \mathbb{R}^2 : qR_{0i} < A < (q+1)R_{0i}, \ q > 0\}. \end{aligned} \tag{2.4}$$

We can check that

$$\Omega = \left\{(I, R) \,|\, 0 \leq I \leq A, \ 0 \leq R \leq qA\right\}$$

is a positively invariant and bounded region for system (2.2).

2.1 Preliminary results

System (2.2) always has a trivial equilibrium $E_0 = (0, 0)$ which corresponds to the disease-free equilibrium $(\frac{b_i}{d_i}, 0, 0)$ of system (1.5). By Zhang et al. (1992), we have the following results.

Lemma 2.2 *The boundary equilibrium $E_0(0, 0)$ of system (2.2) is*

(i.1) *a hyperbolic stable node if $R_{0i} < 1$;*
(i.2) *a saddle-node with a stable parabolic sector in the right (or left) half plane of $\mathbb{R}^2$ if $R_{0i} = 1$, and $p < \frac{1+q}{A}$ (or $p > \frac{1+q}{A}$);*
(i.3) *a stable degenerate node if $R_{0i} = 1$ and $p = \frac{1+q}{A}$;*
(i.4) *a hyperbolic saddle if $R_{0i} > 1$.*

If $E(I, R)$ is a positive equilibrium of system (2.2), then $R = qI$ and hence I satisfies

$$p(q+1)I^2 + (1+q-Ap)I + \frac{A}{R_{0i}} - A = 0 \tag{2.5}$$

in the interval $(0, A)$. The discriminant of (2.5) is

$$\Delta = (1+q-Ap)^2 - 4Ap(q+1)(1-R_{0i})/R_{0i}.$$

Solving $\Delta = 0$ in terms of R_{0i} gives

$$R_0^* = \frac{4Ap(1+q)}{(1+q+Ap)^2}. \tag{2.6}$$

Clearly, $R_0^* \le 1$ with equality if and only if $p = \frac{q+1}{A}$, and $\Delta \ge 0 \Longleftrightarrow R_{0i} \ge R_0^*$. We can see that (2.5) has at most two positive roots, denoted by I_- and I_+, which may coalesce into a unique root I_* if $R_{0i} = R_0^*$, where

$$I_- = \frac{Ap-q-1-\sqrt{\Delta}}{2p(q+1)}, \quad I_+ = \frac{Ap-q-1+\sqrt{\Delta}}{2p(q+1)}, \quad I_* = \frac{Ap-q-1}{2p(q+1)}. \tag{2.7}$$

Correspondingly, system (2.2) has at most two positive equilibria: $E_-(I_-, R_-)$ and $E_+(I_+, R_+)$, which may coalesce into a unique positive equilibrium $E_*(I_*, R_*)$, where $R_- = qI^-$, $R_+ = qI_+$ and $R_* = qI_*$.

The Jacobian matrix of system (2.2) at a positive equilibrium $E(I, R)$ is given by

$$J(E) = \begin{pmatrix} -I\big[1-Ap+pI(2+q)\big] & -I(1+pI) \\ q & -1 \end{pmatrix}.$$

The determinant and trace of $J(E)$ have the same signs as $S_D(I)$ and $S_T(I)$, respectively, where

$$S_D(I) = 2p(1+q)I + 1 + q - Ap, \quad S_T(I) = -1 + (Ap-1)I - p(2+q)I^2. \tag{2.8}$$

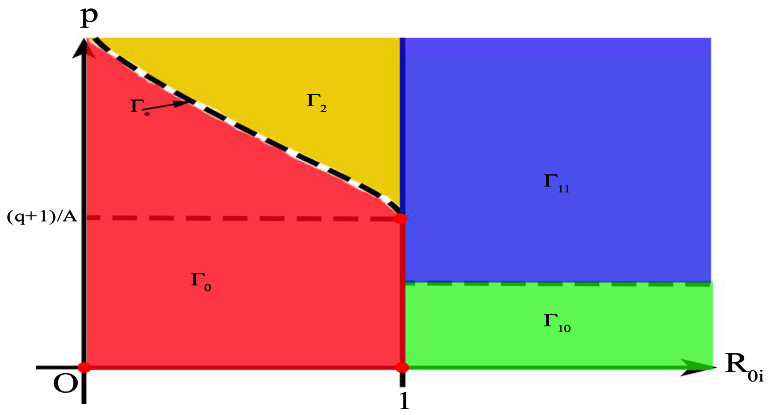

Fig. 1 The partition of (R_{0i}, p)-plane. The number and type of equilibria for system (2.2) at each region are listed in Table 1

Table 1 Number and types of equilibria of system (2.2)

Case	Region	Number	Type
(a)	$\Gamma_0 \times \Lambda$	1	E_0: globally asymptotically stable
(b)	$\Gamma_{10} \times \Lambda$	2	E_0: unstable, E_+: globally asymptotically stable
(c)	$\Gamma_{11} \times \Lambda$	2	E_0: unstable, E_+: elementary and anti-saddle
(d)	$\Gamma_* \times \Lambda$	2	E_0: stable, E_*: degenerate
(e)	$\Gamma_2 \times \Lambda$	3	E_0: stable, E_-: hyperbolic saddle, E_+: elementary and anti-saddle

Define

$$
\begin{aligned}
\Gamma_0 &:= \left\{(R_{0i}, p) \in \mathbb{R}^2 \,|\, 0 < R_{0i} \le 1,\ 0 \le p \le \frac{q+1}{A}\right\} \\
&\quad \bigcup \left\{(R_{0i}, p) \in \mathbb{R}^2 \,|\, 0 < R_{0i} < R_0^*,\ p > \frac{q+1}{A}\right\}, \\
\Gamma_{10} &= \left\{(R_{0i}, p) \in \mathbb{R}^2 \,|\, R_{0i} > 1,\ 0 \le p \le \frac{1}{A}\right\}, \\
\Gamma_{11} &= \left\{(R_{0i}, p) \in \mathbb{R}^2 \,|\, R_{0i} > 1,\ p > \frac{1}{A}\right\} \bigcup \left\{(R_{0i}, p) \in \mathbb{R}^2 \,|\, R_{0i} = 1,\ p > \frac{q+1}{A}\right\}, \\
\Gamma_* &:= \left\{(R_{0i}, p) \in \mathbb{R}^2 \,|\, R_{0i} = R_0^*,\ p > \frac{q+1}{A}\right\}, \\
\Gamma_2 &= \left\{(R_{0i}, p) \in \mathbb{R}^2 \,|\, R_0^* < R_{0i} < 1,\ p > \frac{q+1}{A}\right\}.
\end{aligned} \tag{2.9}
$$

The partition of (R_0^i, p)-plane is illustrated in Fig. 1. We summarize the number of equilibria for system (2.2) and their basic properties in Table 1 (see Jin et al. (2007) for partial results).

Remark 2.3 Following Table 1(a) and (b), and using the original parameters, we have $R_{0i} \le 1 \Longleftrightarrow \beta_i \le \beta_*$, $p \le \frac{1+q}{A} \Longleftrightarrow \nu_i \le \nu_*$, and $R_{0i} \le R_0^* \Longleftrightarrow \beta_i \le \beta^*$, where

$$\beta_* \triangleq \frac{d_i(d_i+\alpha_i)}{b_i}, \quad \nu_* \triangleq \frac{d_i}{b_i}(1+\frac{\alpha_i}{\gamma_i+d_i}), \quad \beta^* \triangleq \beta_* \left(1-\frac{(\nu_i-\nu_*)^2}{(\nu_i+\nu_*)^2}\right). \tag{2.10}$$

The disease will die out for all positive initial conditions if one of the following two cases holds:

(i.1) $\nu_i \le \nu_*$ and $\beta_i \le \beta_*$, i.e., infection rate (due to double exposures) ν_i is smaller than or equal to a critical value ν_* and infection rate (due to single contacts) β_i is smaller than or equal to a critical value β_*;

(i.2) $\nu_i > \nu_*$, $\beta_i < \beta^*$, i.e., ν_i is greater than ν_* and β_i is smaller than a smaller critical value β^*.

The disease will persist in the form of a positive steady state for all positive initial conditions if

(i.3) $\nu_i \le \frac{d_i}{b_i}$ and $\beta_i > \beta_*$, where $\frac{d_i}{b_i} < \nu_*$.

Remark 2.4 When $\nu_i \le \frac{d_i}{b_i}$, Remark 2.3 **(i.1)** and **(i.3)** imply that whether the disease persists or dies out for all positive initial conditions depends on the relative magnitude of β_i and β_*. Thus, when $\nu_i > \frac{d_i}{b_i}$, system (1.5) may exhibits richer dynamics, such as backward bifurcation and Hopf bifurcation.

Next we consider the detailed property of equilibrium E_* for case (d) in Table 1. Let

$$A_* = \frac{(q+1)\sqrt{4p+q}}{p\sqrt{q}}, \quad p_* = \frac{1}{4}\left(q^3+2q^2\right). \tag{2.11}$$

Theorem 2.5 *When $(R_{0i}, p, A, q) \in \Gamma_* \times \Lambda$, system (2.2) has a unique positive equilibrium $E_*(I_*, R_*)$, which is a saddle-node with a stable (or an unstable) parabolic sector if $0 < A < A_*$ (or $A > A_*$). Moreover, when $A = A_*$, E_* is a cusp of codimension 2 if $p \ne p_*$; a cusp of codimension 3 if $p = p_*$.*

Proof **Step 1.** From (2.8), we have $S_D(I_*) = 0$ if $R_{0i} = R_0^*$ and $p > \frac{1+q}{A}$ hold. When $A \ne A_*$, by Zhang et al. (1992), E_* is a saddle-node with a stable (or an unstable) parabolic sector if $0 < A < A_*$ (or $A > A_*$).

Step 2. When $R_{0i} = R_0^*$, $p > \frac{1+q}{A}$ and $A = A_*$ hold, the change of variables

$$I = \frac{1}{q}X + \frac{1}{q}Y + I_*, \quad R = X + R_* \tag{2.12}$$

allow us to rewrite system (2.2) as

$$\begin{aligned} \dot{X} &= Y, \\ \dot{Y} &= \sum_{2 \le i+j \le 3} a_{ij} X^i Y^j. \end{aligned} \tag{2.13}$$

where

$$a_{20} = -\frac{(q+1)\left(\sqrt{4p+q}-\sqrt{q}\right)}{2q^{3/2}}, \quad a_{11} = -\frac{\sqrt{4p+q}}{q^{3/2}} + \frac{1}{q} + 1,$$

$$a_{02} = \frac{q\sqrt{4p+q} - \sqrt{4p+q} + q^{3/2} + \sqrt{q}}{2q^{3/2}},$$
$$a_{30} = -\frac{p(q+1)}{q^2}, \quad a_{21} = -\frac{p(2q+3)}{q^2}, \quad a_{12} = -\frac{p(q+3)}{q^2}, \quad a_{03} = -\frac{p}{q^2}. \tag{2.14}$$

By introducing

$$X = x + \frac{a_{02}}{2}x^2, \quad Y = y + a_{02}xy,$$

system (2.13) becomes

$$\begin{aligned} \dot{x} &= y, \\ \dot{y} &= b_{20}x^2 + b_{11}xy + \sum_{3\le i+j\le 4} b_{ij}x^i y^j + o(|x,y|^4). \end{aligned} \tag{2.15}$$

where

$$b_{20} = -\frac{(q+1)\left(\sqrt{4p+q} - \sqrt{q}\right)}{2q^{3/2}} \quad \text{and} \quad b_{11} = -\frac{\sqrt{4p+q}}{q^{3/2}} + \frac{1}{q} + 1,$$

and other expressions of b_{ij} are omitted here for brevity. Obviously, $b_{20} < 0$. Direct computation shows that $b_{11} = 0$ if $p = p_*$. Therefore, E_* is a cusp of codimension 2 if $p \neq p_*$.

Step 3. When $R_{0i} = R_0^*$, $p > \frac{1+q}{A}$, $A = A_*$ and $p = p_*$, we shall prove that E_* is a cusp of codimension at most 3. Following Lemma 2.4 in Lu et al. (2023), system (2.15) near the origin is equivalent to the following system

$$\begin{aligned} \dot{x} &= y, \\ \dot{y} &= x^2 + \tfrac{q(q+2)}{4\sqrt{2}\sqrt{q+1}}x^3 y + o(|x,y|^4). \end{aligned} \tag{2.16}$$

This completes the proof. □

Remark 2.6 It follows from Theorem 2.5 that the chance of disease outbreak depends on ν_i, the recovery rate α_i and the initial conditions. More precisely, when $\beta_i = \beta^*$ and $\nu_i > \nu_*$ i.e., $(R_{0i}, p, A, q) \in \Gamma_* \times \Lambda$, system (1.5) has two equilibria: a disease-free equilibrium E_0 and an endemic equilibrium E_*. Moreover, the disease will die out for almost all positive initial conditions if $\alpha_i > \alpha_*$ and $\nu_i \geq \nu^*$ (i.e. $A \geq A_*$), where

$$\begin{aligned} \alpha_* &\triangleq \frac{1}{2}\left(\gamma_i + \sqrt{5\gamma_i^2 + 4d_i^2 + 8\gamma_i d_i}\right), \\ \nu^* &\triangleq \nu_* \frac{\alpha_i(\alpha_i + d_i) + (d_i + \gamma_i)(d_i + \gamma_i + \alpha_i)}{\alpha_i(\alpha_i + d_i) - (d_i + \gamma_i)(d_i + \gamma_i + \alpha_i)}. \end{aligned} \tag{2.17}$$

Otherwise, the disease will persist in the form of a positive steady state for some positive initial conditions if $\alpha_i \leq \alpha_*$, or $\alpha_i > \alpha_*$ and $\nu_i < \nu^*$ (i.e., $A < A_*$).

2.2 Degenerate Bogdanov–Takens bifurcation of codimension 3

From Theorem 2.5, we know that system (2.2) may exhibit Bogdanov–Takens bifurcation of codimension 3 around $E_*(I_*, R_*)$. In this section, we will explore rigorously whether a Bogdanov–Takens bifurcation of codimension 3 can be fully unfolded inside the class of system (2.2). We choose R_{0i}, A and p as bifurcation parameters, and consider the following unfolding system

$$\begin{aligned} \frac{dI}{dt} &= I(1+(p_*+r_3)I)(A_*+r_2-I-R)-\frac{A_*+r_2}{R_0^*+r_1}I, \\ \frac{dR}{dt} &= qI-R, \end{aligned} \tag{2.18}$$

where $r=(r_1,r_2,r_3)\sim(0,0,0)$.

Theorem 2.7 *System (2.2) can undergo degenerate Bogdanov–Takens bifurcation of codimension 3 around E_* as (R_{0i}, A, p) varies near (R_0^*, A_*, p_*). There exist two limit cycles appearing in a Hopf bifurcation of codimension 2 and dying in a homoclinic bifurcation of codimension 2. The cusp of codimension 3 is the organizing center of bifurcation sets, i.e., there exist a series of bifurcations with lower codimension: codimension-1: saddle-node, Hopf, homoclinic bifurcations and bifurcation of a double limit cycle; codimension-2: Bogdanov–Takens bifurcation, degenerate Hopf bifurcation, degenerate homoclinic bifurcation, simultaneous occurrence of Hopf and homoclinic bifurcation.*

Proof First, let $(I, R)=(\frac{1}{q}X+\frac{1}{q}Y+I_*, X+R_*)$, system (2.18) becomes

$$\begin{aligned} \dot{X} &= Y, \\ \dot{Y} &= \sum_{0\le i+j\le 3}\bar{a}_{ij}X^iY^j, \end{aligned} \tag{2.19}$$

where

$$\begin{aligned} \bar{a}_{00} &= \frac{(q+2)^2}{2q^2}r_1+\frac{q}{2q+2}r_2+\frac{8(q+1)}{q^3(q+2)^2}r_3+O(r^2), \\ \bar{a}_{10} &= \frac{(q+2)^3}{4q^2}r_1+\frac{q(3q+4)}{4(q+1)}r_2+\frac{4(q+1)(q+4)}{q^3(q+2)^2}r_3+O(r^2), \\ \bar{a}_{01} &= \frac{(q+2)^3}{4q^2}r_1+\frac{q(3q+4)}{4(q+1)}r_2+\frac{4\left(2q^2+5q+4\right)}{q^3(q+2)^2}r_3+O(r^2), \\ \bar{a}_{11} &= \frac{1}{2}q(q+2)r_2+\frac{4}{q^3}r_3+O(r^2), \\ \bar{a}_{20} &= \frac{1}{2}(-q-1)+O(r), \quad \bar{a}_{02}=\frac{q+1}{2}+O(r), \\ \bar{a}_{30} &= -\frac{1}{4}(q+1)(q+2)+O(r), \\ \bar{a}_{21} &= -\frac{1}{4}(q+2)(2q+3)+O(r), \quad \bar{a}_{12}=-\frac{1}{4}(q+2)(q+3)+O(r), \end{aligned}$$

$$\bar{a}_{03} = \frac{1}{4}(-q-2) + O(r).$$

Next, following similar steps as in Arsie et al. (2022), Li et al. (2015) and Xiang et al. (2019) and performing a sequence of near-identity transformations and time rescaling (preserving orientations of orbits), we can reduce system (2.19) to the following form:

$$\begin{aligned} \frac{dx_1}{dt} &= y_1, \\ \frac{dy_1}{dt} &= \gamma_1 + \gamma_2 y_1 + \gamma_3 x_1 y_1 + x_1^2 + x_1^3 y_1 + R(x_1, y_1, r), \end{aligned} \tag{2.20}$$

where $R(x_1, y_1, r) = y_1^2 O(|x_1, y_1|^2) + O(|x_1, y_1|^5) + O(r)(O(y_1^2) + O(|x_1, y_1|^3)) + O(r^2)O(|x_1, y_1|)$.

A direct but tedious algebraic computation shows that

$$\left| \frac{\partial(\gamma_1, \gamma_2, \gamma_3)}{\partial(r_1, r_2, r_3)} \right|_{r=0} = -\frac{(q+2)^5}{2(-q-1)^{17/5}(-q(q+2))^{11/5}} < 0$$

due to $q > 0$. Therefore, by the results of Dumortier et al. (1987) and Chow et al. (1994), we know that system (2.20) is the versal unfolding of Bogdanov–Takens singularity (cusp case) of codimension 3. The remainder term $R(x_1, y_1, r)$ has no influence on the bifurcation analysis. □

Remark 2.8 In Jin et al. (2007), Jin et al. only showed the existence of Bogdanov–Takens bifurcation of codimension 2. In this paper, we have shown that the highest codimension of the cusp E_* is 3, and system (2.2) can undergo degenerate Bogdanov–Takens bifurcation of codimension 3.

2.3 Hopf bifurcation with codimension up to 2

From Table 1 (c) and (e), we know that $E_+(I_+, R_+)$ is an elementary and anti-saddle equilibrium. In Theorem 3.1 of Jin et al. (2007), Jin et al. found that the positive equilibrium $E_+(I_+, R_+)$ can be a center-type equilibrium if $S_T(I_+) = 0$, and discussed the existence of Hopf bifurcation of codimension 1. However, is it a center or focus when $S_T(I_+) = 0$? What is the exact order of E_+ when it is a weak focus? Can system (2.2) exhibit Hopf bifurcation with corresponding order? These problems related to the number of small-amplitude limit cycles remain open.

In this subsection, we show that $E_+(I_+, R_+)$ is a weak focus with multiplicity at most 2 if $S_T(I_+) = 0$, and system (2.2) can undergo Hopf bifurcation of codimension 2. To simplify the notation, we denote $I_+ \triangleq x$ and

$$F(x) \triangleq p(q+1)x^2 + (1+q-Ap)x + \frac{A}{R_{0i}} - A. \tag{2.21}$$

Then $(I_+, R_+) = (x, qx)$. From $F(x) = 0$ in (2.21) and $S_T(x) = 0$ in (2.8), we can express R_{0i} and A by p, q and x as follows

$$R_{0i} = R_0^H := \frac{A}{(px+1)(A-qx-x)} \quad \text{and} \quad A = A^H := \frac{pqx^2+2px^2+x+1}{px}. \tag{2.22}$$

From the above and (2.8), we have

$$\mathrm{Det}(x) := xS_D(x) = qx(px+1) - 1. \tag{2.23}$$

It can be shown that $F(x) = 0$, $S_T(x) = 0$ and $(R_{0i}, p, A, q) \in \Gamma \times \Lambda \iff (R_{0i}, p, A, q, x) \in D$, where

$$D = \left\{ (R_{0i}, p, A, q, x) \in \mathbb{R}^5_+ \mid R_{0i} = R_0^H, \right.$$
$$\left. A = A^H, \ \frac{p^2x^3+2px^2+x+1}{px} < q < \frac{p^2x^3+2px^2+px+x+1}{px} \right\}.$$

Similarly, $F(x) = 0$, $S_T(x) = 0$ and $(R_{0i}, p, A, q) \in \Gamma_{11} \times \Lambda$ (or $\Gamma_2 \times \Lambda$) $\iff (R_{0i}, p, A, q, x) \in D_1$ (or D_2), where

$$D_1 \triangleq \left\{ (R_{0i}, p, A, q, x) \in \mathbb{R}^5_+ \,\middle|\, q \geq \frac{1+px^2}{x} \right\} \cap D,$$
$$D_2 \triangleq \left\{ (R_{0i}, p, A, q, x) \in \mathbb{R}^5_+ \,\middle|\, \frac{1}{x(px+1)} < q < \frac{1+px^2}{x} \right\} \cap D. \tag{2.24}$$

We next compute the first two focal values of system (2.2) around E_+ when $(R_{0i}, p, A, q, x) \in D_1$ (or D_2), under which $\mathrm{Det}(x) > 0$. With the following transformations

$$I = 2y_1 + x, \quad R = \frac{2y_1}{x(px+1)} + \frac{2\sqrt{qx(px+1)-1}}{x(px+1)} y_2 + qx, \quad \text{and} \quad t = \frac{\tau}{\sqrt{\mathrm{Det}(x)}},$$

then system (2.2) becomes (still denote τ by t)

$$\begin{aligned}
\frac{dy_1}{dt} &= -y_2 - \frac{2p\left(px^2+x+1\right)}{(px+1)\sqrt{\mathrm{Det}(x)}} y_1^2 - \frac{2(2px+1)}{x(px+1)} y_1 y_2 \\
&\quad - \frac{4p\left(px^2+x+1\right)}{x(px+1)\sqrt{\mathrm{Det}(x)}} y_1^3 - \frac{4p}{x(px+1)} y_1^2 y_1, \\
\frac{dy_2}{dt} &= y_1 + \frac{2p\left(px^2+x+1\right)}{(px+1)\mathrm{Det}(x)} y_1^2 + \frac{2(2px+1)}{x(px+1)\sqrt{\mathrm{Det}(x)}} y_1 y_2 \\
&\quad + \frac{4p\left(px^2+x+1\right)}{x(px+1)\mathrm{Det}(x)} y_1^3 + \frac{4p}{x(px+1)\sqrt{\mathrm{Det}(x)}} y_1^2 y_1.
\end{aligned} \tag{2.25}$$

According to successive function method (Chow et al. 1994), we get the first focal value

$$\sigma_1 = \frac{p\left(2p^2x^3+p(2x+3)x+1-q\left(p^2x^3+3px^2+2x+1\right)\right)}{2(px+1)(\mathrm{Det}(x))^{3/2}}. \tag{2.26}$$

Obviously, σ_1 has the same sign as

$$\sigma_{11} := 2p^2x^3 + p(2x+3)x + 1 - q\left(p^2x^3 + 3px^2 + 2x + 1\right).$$

When $(R_{0i}, p, A, q, x) \in D_1$, we have $\sigma_{11} < 0$, then E_+ is a stable weak focus with order 1. When $(R_{0i}, p, A, q, x) \in D_2$, solving $\sigma_{11} = 0$ with respect to q gives

$$q = q^H \triangleq \frac{2p^2x^3 + 2px^2 + 3px + 1}{p^2x^3 + 3px^2 + 2x + 1}, \tag{2.27}$$

and we obtain the second focal value

$$\sigma_2 = \frac{p^2\left(px^2+x+1\right)^2\left(2p^2x^3+2px^2-1\right)\left(3p^3x^4+9p^2x^3+6px^2+6px+2\right)}{3x(px+1)^2\left(p^2x^3+3px^2+2x+1\right)^2(\mathrm{Det}(x))^{5/2}} > 0,$$

since $(R_{0i}, p, A, q, x) \in D_2$ and $q = q^H$.

Moreover, we have

$$\left.\frac{dS_T(x)}{dA}\right|_{A=A^H} = px > 0, \quad \left.\frac{d\sigma_{11}}{dq}\right|_{q=q^H} = -\left(p^2x^3 + 3px^2 + 2x + 1\right) < 0,$$

and

$$\det\left(\frac{\partial(S_T(x), \sigma_{11})}{\partial(A, q)}\right)\Big|_{A=A^H, q=q^H} = -px\left(p^2x^3 + 3px^2 + 2x + 1\right) < 0.$$

then we can get the following results.

Theorem 2.9 (I) *When $(R_{0i}, p, A, q, x) \in D_1$, E_+ is a stable weak focus with order 1, and system (2.2) can exhibit supercritical Hopf bifurcation.*

(II) *When $(R_{0i}, p, A, q, x) \in D_2$, E_+ is a weak focus with order at most 2. Moreover,*

(i) *if $q > q^H$, then E_+ is a stable weak focus with order 1, and system (2.2) can exhibit supercritical Hopf bifurcation;*

(ii) *if $q < q^H$, then E_+ is an unstable weak focus with order 1, and system (2.2) can exhibit subcritical Hopf bifurcation;*

(iii) *if $q = q^H$, then E_+ is an unstable weak focus with order exactly 2, and system (2.2) can undergo Hopf bifurcation of codimension 2. Thus, system (2.2) has two limit cycles (the inner one is stable).*

Remark 2.10 The existence of a stable limit cycle arising from supercritical Hopf bifurcation around E_+ in system (2.2) is given in Fig. 2a, where $x = 1$, $p = 8$,

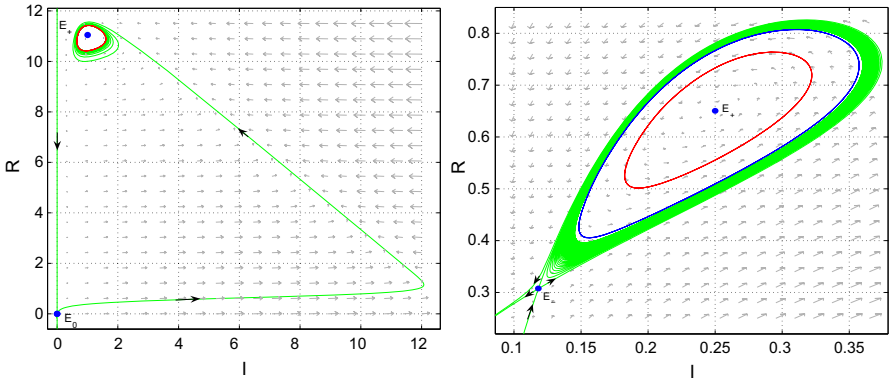

Fig. 2 **a** A stable limit cycle of system (2.2). **b** Two limit cycles of system (2.2) (the inner one is stable)

$q = 11$, $A = \frac{53}{4} + \frac{1}{10}$, $R_{0i} = \frac{133}{117}$. The existence of two limit cycles arising from degenerate Hopf bifurcation of codimension 2 around E_+ in system (2.2) is given in Fig. 2b, where the inner one is stable, $x = \frac{1}{4}$, $p = 8$, $q = \frac{5}{2} + \frac{1}{10}$, $A = \frac{71}{40} + \frac{4}{10000}$, $R_{0i} = \frac{2959}{4377}$.

Remark 2.11 From Theorem 2.9 and (2.10), if $\beta_i > \beta_*$ and $\nu_i \geq \frac{d_i}{b_i}$, or $\beta_i = \beta_*$ and $\nu_i > \nu_*$ (i.e., $(R_{0i}, p, A, q) \in \Gamma_{11} \times \Lambda$), then system (1.5) may exhibit supercritical Hopf bifurcation, crossing which a stable limit cycle arising, at this moment, disease-free equilibrium E_0 and the unique endemic equilibrium E_+ are both unstable. Thus, the disease will tend to stable periodic outbreaks for almost all positive initial conditions.

Remark 2.12 From Theorem 2.9, Fig. 2b and (2.10), we can see that, if $\beta^* < \beta_i < \beta_*$ and $\nu_i > \nu_*$ (i.e., $(R_{0i}, p, A, q) \in \Gamma_2 \times \Lambda$), then E_0 is stable, E_- is a saddle, E_+ may be stable or unstable, system (1.5) may have a stable or an unstable limit cycle, or two limit cycles around E_+. There exist two kinds of bistability: E_0 and E_+, or E_0 and a limit cycle. Whether the disease dies out or persists will not only depends on more parameters but also on the initial conditions.

3 Dynamics in connected environment

The total population size in two patches is $N(t) = N_1(t) + N_2(t)$. Let

$$X = \{(S_1, I_1, R_1, S_2, I_2, R_2) : S_i \geq 0,\ I_i \geq 0,\ R_i \geq 0, i = 1, 2\}.$$

The model (1.1) is mathematically and epidemiologically well-posed in the domain X.

Theorem 3.1 *There exists a unique solution, defined for all time $t \geq 0$, for system (1.1) with $S_i(0) \geq 0$, $I_i(0) \geq 0$ and $R_i(0) \geq 0$. Moreover, X is positively invariant with respect to (1.1), and the total population $N(t)$ is bounded.*

Proof The uniqueness and nonnegativity of state variables can be easily checked. By a comparison principle, the fact

$$b_1 + b_2 - \max\{d_1, d_2\}N \leq \frac{dN}{dt} = b_1 + b_2 - d_1N_1 - d_2N_2 \leq b_1 + b_2 - \min\{d_1, d_2\}N$$

implies $N(t)$ is bounded above by $\max\left\{\frac{b_1+b_2}{\min\{d_1,d_2\}}, N(0)\right\}$ and below by $\min\left\{\frac{b_1+b_2}{\max\{d_1,d_2\}}, N(0)\right\}$. □

3.1 Threshold dynamics

For system (1.1), there always exists a disease-free equilibrium $E^0 = (S_{10}, 0, 0, S_{20}, 0, 0)$, where

$$S_{10} = \frac{b_2M_{21}^S + b_1M_{21}^S + b_1d_2}{d_2M_{12}^S + d_1M_{21}^S + d_1d_2}, \quad S_{20} = \frac{b_2M_{12}^S + b_1M_{12}^S + d_1b_2}{d_2M_{12}^S + d_1M_{21}^S + d_1d_2}. \tag{3.1}$$

We first consider the local stability of E^0. Following the next generation matrix method in Diekmann et al. (2010) and van den Driessche and Watmough (2002), we have

$$F = \begin{pmatrix} \beta_1 S_{10} & 0 \\ 0 & \beta_2 S_{20} \end{pmatrix}, \quad V = \begin{pmatrix} d_1 + \alpha_1 + b_{12} & -b_{21} \\ -b_{12} & d_2 + \alpha_2 + b_{21} \end{pmatrix},$$

and

$$FV^{-1} = \frac{1}{\Pi_0}\begin{pmatrix} \Pi_{11}S_{10} & \Pi_{12}S_{10} \\ \Pi_{21}S_{20} & \Pi_{22}S_{20} \end{pmatrix},$$

where

$$\begin{aligned} &\Pi_0 = (d_2 + \alpha_2 + b_{21})(d_1 + \alpha_1 + b_{12}) - b_{21}b_{12}, \quad \Pi_{11} = \beta_1(d_2 + \alpha_2 + b_{21}), \\ &\Pi_{12} = \beta_1 b_{21}, \quad \Pi_{21} = \beta_2 b_{12}, \quad \Pi_{22} = \beta_2(d_1 + \alpha_1 + b_{12}). \end{aligned} \tag{3.2}$$

The basic reproduction number of model (1.1) is

$$R_0 = \rho(FV^{-1}) = \frac{\Pi_{11}S_{10} + \Pi_{22}S_{20} + \sqrt{(\Pi_{11}S_{10} - \Pi_{22}S_{20})^2 + 4\Pi_{12}S_{10}\Pi_{21}S_{20}}}{2\Pi_0}, \tag{3.3}$$

where ρ is the spectral radius of a square matrix.

Remark 3.2 Note that R_0 in (3.3) depends on the travel rates of susceptible and infective individuals (M_{ij}^S and b_{ij}), but it is independent of the travel rates of recovered individuals (M_{ij}^R), and the parameters γ_i and ν_i. Moreover,

(1) if the infective individuals in patch 1 do not travel to patch 2, i.e., $b_{12} = 0$, then $R_0 = \max\left\{\frac{\beta_1 S_{10}}{d_1+\alpha_1}, \frac{\beta_2 S_{20}}{d_2+\alpha_2+b_{21}}\right\}$, which depends on the travel rates M_{ij}^S and b_{21};
(2) if the infective individuals in patch 2 do not travel to patch 1, i.e., $b_{21} = 0$, then $R_0 = \max\left\{\frac{\beta_1 S_{10}}{d_1+\alpha_1+b_{12}}, \frac{\beta_2 S_{20}}{d_2+\alpha_2}\right\}$, which depends on the travel rates M_{ij}^S and b_{12};
(3) if the infective individuals do not travel between two patches, i.e., $b_{12} = b_{21} = 0$, then $R_0 = \max\left\{\frac{\beta_1 S_{10}}{d_1+\alpha_1}, \frac{\beta_2 S_{20}}{d_2+\alpha_2}\right\}$, which depends on the travel rates M_{ij}^S.

Remark 3.3 If the disease transmission is depicted by standard incidence: $\beta_i \frac{S_i}{N_i} I_i$, then

$$R_0 = \frac{\Pi_{11} + \Pi_{22} + \sqrt{(\Pi_{11} - \Pi_{22})^2 + 4\Pi_{12}\Pi_{21}}}{2\Pi_0}, \tag{3.4}$$

which does not depend on the travel rates of susceptible and recovered individuals. Moreover, if the infective individuals does not move between patches, i.e., $b_{12} = b_{21} = 0$, then $R_0 = \max\left\{\frac{\beta_1}{d_1+\alpha_1}, \frac{\beta_2}{d_2+\alpha_2}\right\}$, which is unaffected by the travel rates. Thus, the dependence of $\mathbb{R}_0$ on travel rates becomes more complex when the incidence rate is nonstandard.

Following Theorem 2 in van den Driessche and Watmough (2002), we immediately have the following result on the local stability of the disease-free equilibrium.

Lemma 3.4 *The disease-free equilibrium E^0 of system (1.1) is locally asymptotically stable if $R_0 < 1$ and unstable if $R_0 > 1$.*

We next consider the global asymptotic stability of E^0 of system (1.1) under the case where the travel rates are independent of disease status and disease prevalence, i.e., $\theta_{ij}^S = \theta_{ij}^R = 0$ and $M_{ij}^S = M_{ij}^R = b_{ij}$ for $i, j = 1, 2, i \neq j$, and infections due to double exposures are ignored, i.e., $\nu_i = 0$ for $i = 1, 2$. For example, a disease like the common cold has a mild effect on the mobility of infected individuals.

Theorem 3.5 *The disease-free equilibrium E^0 of system (1.1) is globally asymptotically stable in X, i.e., the disease becomes extinct in two patches, if $R_0 < 1$, $\theta_{ij}^S = \theta_{ij}^R = 0$, $M_{ij}^S = M_{ij}^R = b_{ij}$ and $\nu_i = 0$ for $i, j = 1, 2, i \neq j$.*

Proof When $\theta_{ij}^S = \theta_{ij}^R = 0$, $M_{ij}^S = M_{ij}^R = b_{ij}$, $i, j = 1, 2, i \neq j$, the total population sizes in patches 1 and 2 satisfy

$$\frac{dN_1}{dt} = b_1 - d_1 N_1 - b_{12} N_1 + b_{21} N_2,$$

$$\frac{dN_2}{dt} = b_2 - d_2N_2 + b_{12}N_1 - b_{21}N_2. \tag{3.5}$$

System (3.5) has a unique equilibrium $(N_1^*, N_2^*) = (S_{10}, S_{20})$, which is a stable node. It is easy to show that (N_1^*, N_2^*) is globally asymptotically stable for $(N_1, N_2) \in \mathbb{R}^2_+$. It then follows that for any given $\epsilon > 0$, we have $S_i(t) \le N_i(t) < S_{i0} + \epsilon$ $(i = 1, 2)$ for sufficiently large t. Thus, if t is sufficiently large and $v_i = 0$, we have

$$\begin{aligned}
\frac{dI_1}{dt} &\le [\beta_1(S_{10} + \epsilon) - (d_1 + \alpha_1 + b_{12})]I_1 + b_{21}I_2,\\
\frac{dI_2}{dt} &\le b_{12}I_1 + [\beta_2(S_{20} + \epsilon) - (d_2 + \alpha_2 + b_{21})]I_2.
\end{aligned} \tag{3.6}$$

Define an auxiliary linear system:

$$\begin{aligned}
\frac{d\bar{I}_1}{dt} &= [\beta_1(S_{10} + \epsilon) - (d_1 + \alpha_1 + b_{12})]\bar{I}_1 + b_{21}\bar{I}_2,\\
\frac{d\bar{I}_2}{dt} &= b_{12}\bar{I}_1 + [\beta_2(S_{20} + \epsilon) - (d_2 + \alpha_2 + b_{21})]\bar{I}_2,
\end{aligned} \tag{3.7}$$

or equivalently,

$$\frac{d}{dt}\begin{pmatrix}\bar{I}_1\\ \bar{I}_2\end{pmatrix} = (F - V + \epsilon D)\begin{pmatrix}\bar{I}_1\\ \bar{I}_2\end{pmatrix}$$

with $D = \mathrm{diag}(\mathrm{fi}_1, \mathrm{fi}_2)$. We have $R_0 < 1 \Longleftrightarrow \sigma(F - V) < 0$, where $\sigma(M)$ is the stability modulus of matrix M [see van den Driessche and Watmough (2002)]. Thus, when $R_0 < 1$, we can fix an $\epsilon > 0$ small enough such that $\sigma(F - V + \epsilon D) < 0$, since $\sigma(F - V + \epsilon D)$ is continuous for small ϵ. Then all non-negative solutions of system (3.7) satisfy $\lim_{t\to\infty} \bar{I}_i = 0$ $(i = 1, 2)$. By a standard comparison principle and the nonnegativity of I_i, when $R_0 < 1$, all non-negative solutions of (1.1) satisfy $\lim_{t\to\infty} I_i = 0$ $(i = 1, 2)$. Then we have

$$\begin{aligned}
\frac{dR_1}{dt} &= -(d_1 + \gamma_1)R_1 - b_{12}R_1 + b_{21}R_2,\\
\frac{dR_2}{dt} &= -(d_2 + \gamma_2)R_2 + b_{12}R_1 - b_{21}R_2.
\end{aligned} \tag{3.8}$$

This linear system has a unique equilibrium $(0, 0)$, which is globally asymptotically stable. Thus $\lim_{t\to\infty} R_i = 0$ $(i = 1, 2)$. Since I_i and R_i tend to 0 as $t \to \infty$, system (1.1) is an asymptotically autonomous system with limit affine system

$$\begin{aligned}
\frac{dS_1}{dt} &= b_1 - d_1S_1 - b_{12}S_1 + b_{21}S_2,\\
\frac{dS_2}{dt} &= b_2 - d_2S_2 + b_{12}S_1 - b_{21}S_2,
\end{aligned} \tag{3.9}$$

from which $\lim_{t\to\infty} S_i = S_{i0}$ $(i = 1, 2)$ is obvious. The proof is complete. □

On the other hand, $R_0 > 1$ actually implies that system (1.1) admits at least one endemic equilibrium and the disease is uniformly persistent.

Theorem 3.6 *When $R_0 > 1$ and $b_{ij} > 0$ $(i, j = 1, 2, i \neq j)$, system (1.1) is uniformly persistent, namely, there exists a positive constant ϵ such that every solution $\phi_t(\mathrm{x}_0) \equiv (S_1(t), I_1(t), R_1(t), S_2(t), I_2(t), R_2(t))$ of (1.1) satisfies*

$$\liminf_{t\to\infty} S_i(t) \geq \epsilon, \quad \liminf_{t\to\infty} I_i(t) \geq \epsilon, \quad \liminf_{t\to\infty} R_i(t) \geq \epsilon, \quad i = 1, 2,$$

for initial condition $\mathrm{x}_0 \equiv (S_1(0), I_1(0), R_1(0), S_2(0), I_2(0), R_2(0)) \in X$ satisfying $I_1(0) + I_2(0) > 0$, and system (1.1) admits at least one endemic equilibrium.

Proof Clearly, $S_i(t)$ is always ultimately lower bounded by some positive constant, which is independent of initial values. If both I_1 and I_2 are ultimately lower bounded by some positive constant independent of initial values, then R_i is also ultimately lower bounded by some positive constant which is independent of initial values. Therefore it suffices to prove that $\liminf_{t\to\infty} I_i(t) \geq \epsilon$, $i = 1, 2$.

Let

$$X_0 = \{(S_1, I_1, R_1, S_2, I_2, R_2) \in X : I_1 > 0, I_2 > 0\},$$
$$\partial X_0 = X \setminus X_0 = \{(S_1, I_1, R_1, S_2, I_2, R_2) \in X : I_1 = 0 \text{ or } I_2 = 0\}.$$

It then suffices to show that system (1.1) is uniformly persistent with respect to $(X_0, \partial X_0)$, i.e., there exists $\eta > 0$, such that $\liminf_{t\to\infty} d(\phi_t(\mathrm{x}_0), \partial X_0) \geq \eta$ for $\mathrm{x}_0 \in X_0$ (see Thieme (1993), Zhao (2003)). Clearly, ∂X_0 is relatively closed in X, and X, X_0 are positive invariant. Denote

$$M_\partial = \{\mathbf{x}_0 \in \partial X_0 : \phi_t(\mathbf{x}_0) \in \partial X_0 \text{ for } t \geq 0\},$$
$$X_1 = \{\mathbf{x}_0 \in X : I_1(0) = I_2(0) = 0\}.$$

We now show that $M_\partial = X_1$. Obviously, $X_1 \subset M_\partial$. On the other hand, we have $I_1(0) + I_2(0) > 0$ for any $\mathbf{x}_0 \in \partial X_0 \setminus X_1$. Without losing generality, we assume $I_1(0) > 0$ and $I_2(0) = 0$. If $b_{12} > 0$, then

$$\left.\frac{dI_2}{dt}\right|_{t=0} = b_{12} I_1(0) > 0. \tag{3.10}$$

It follows that there exits a $\delta_0 > 0$ such that $I_2(t) > 0$ for $t \in (0, \delta_0)$. Moreover, we can restrict δ_0 to be small enough such that $I_1(t) > 0$ for $t \in (0, \delta_0)$. Thus, $\phi_t(\mathbf{x}_0) \in X_0$ for $t \in (0, \delta_0)$, then $\mathbf{x}_0 \notin M_\partial$. Therefore, $M_\partial \subset X_1$, which implies that $M_\partial = X_1$.

Restricting system (1.1) on M_∂ gives

$$\begin{aligned}
\frac{dS_1}{dt} &= b_1 - d_1 S_1 + \gamma_1 R_1 - M_{12}^S S_1 + M_{21}^S S_2,\\
\frac{dR_1}{dt} &= -(d_1+\gamma_1)R_1 - M_{12}^R R_1 + M_{21}^R R_2,\\
\frac{dS_2}{dt} &= b_2 - d_2 S_2 + \gamma_2 R_2 + M_{12}^S S_1 - M_{21}^S S_2,\\
\frac{dR_2}{dt} &= -(d_2+\gamma_2)R_2 + M_{12}^R R_1 - M_{21}^R R_2,
\end{aligned} \tag{3.11}$$

It is easy to verify that system (3.11) has a unique equilibrium $E_1(S_{10}, 0, S_{20}, 0)$. Thus, the disease free equilibrium E^0 is the unique equilibrium of system (1.1) on M_∂. It is easy to check that E_1 of system (3.11) is locally asymptotically stable. Hence it is also globally asymptotically stable since system (3.11) is linear. Denote the omega limit set of the solutions of system (1.1) with $\mathbf{x}_0 \in M_\partial$ by $\omega(\mathbf{x}_0)$. Thus, $\underset{\mathbf{x}_0\in M_\partial}{\cup} \omega(\mathbf{x}_0) = \{E^0\}$. E^0 is isolated (since E^0 is the unique equilibrium) and is acyclic (since there exists no solution on M_∂ which links E^0 to itself).

Let $W^s(E^0)$ be the stable manifold of E^0. We now show that $W^s(E^0) \cap X_0 = \emptyset$ when $R_0 > 1$. Suppose not, then there exists a solution $\phi_t(\mathbf{x}_0) \in X_0$ for $t \geq 0$ with initial value $\mathbf{x}_0 \in X_0$ such that

$$\lim_{t\to\infty} \phi_t(\mathbf{x}_0) = E^0,\ i = 1, 2. \tag{3.12}$$

Namely, for any fixed $\delta > 0$, there exists $t_1 > 0$ such that

$$S_{i0} - \delta < S_i(t) < S_{i0} + \delta,\ 0 < I_i(t) < \delta,\ 0 < R_i(t) < \delta,\ \ t \geq t_1,\ i = 1, 2. \tag{3.13}$$

Hence

$$\begin{aligned}
\frac{dI_1}{dt} &\geq \beta_1 I_1(S_{10} - \delta) - (d_1 + \alpha_1)I_1 - b_{12}I_1 + b_{21}I_2,\\
\frac{dI_2}{dt} &\geq \beta_2 I_2(S_{20} - \delta) - (d_2 + \alpha_2)I_2 + b_{12}I_1 - b_{21}I_2.
\end{aligned} \tag{3.14}$$

Define an auxiliary linear system:

$$\begin{aligned}
\frac{d\bar{I}_1}{dt} &= [\beta_1(S_{10} - \delta) - (d_1 + \alpha_1 + b_{12})]\bar{I}_1 + b_{21}\bar{I}_2,\\
\frac{d\bar{I}_2}{dt} &= b_{12}\bar{I}_1 + [\beta_2(S_{20} - \delta) - (d_2 + \alpha_2 + b_{21})]\bar{I}_2,
\end{aligned} \tag{3.15}$$

i.e.,

$$\frac{d}{dt}\begin{pmatrix}\bar{I}_1\\ \bar{I}_2\end{pmatrix} = (F - V - \delta D)\begin{pmatrix}\bar{I}_1\\ \bar{I}_2\end{pmatrix}$$

Table 2 Parameter values of system (1.1)

Parameter	b_1	b_2	d_1	d_2	α_1	α_2	γ_1	γ_2	ν_1	ν_2
Value	1000	200	0.001	0.002	0.8	0.5	0.1	0.1	0	0

with $D = \mathrm{diag}(\mathrm{fi}_1, \mathrm{fi}_2)$. Since $R_0 > 1 \Longleftrightarrow \sigma(F-V) > 0$, where $\sigma(M)$ is the stability modulus of matrix M (see van den Driessche and Watmough (2002)). Thus, when $R_0 > 1$, we can fix an $\delta_1 > 0$ small enough such that $\sigma(F - V - \delta D) > 0$ for $0 \le \delta \le \delta_1$. Notice that $F-V-\delta D$ has a positive eigenvalue $\sigma(F-V-\delta D)$ associated to a positive eigenvector. It follows from a comparison theorem that $\lim_{t\to\infty} I_i(t) = \infty$ $(i = 1, 2)$, which induces to a contradiction. By Theorem 4.6 in Thieme (1993), system (1.1) is uniformly persistent with respect to $(X_0, \partial X_0)$.

A continuous mapping $f : X \to X$ is dissipative if there is a bounded set B_0 in X such that B_0 attracts each point in X. Theorem 3.1 implies that $\phi_t(\mathbf{x}_0)$ is point dissipative. Therefore, by Theorem 2.4 in Zhao (1995), we know that system has an equilibrium $\bar{E} = (\bar{S}_1, \bar{I}_1, \bar{R}_1, \bar{S}_2, \bar{I}_2, \bar{R}_2) \in X_0$. The differential equations governing S_i and R_i ensure that $\bar{S}_i > 0$ and $\bar{R}_i > 0$ for $i = 1, 2$. This means that $\bar{E}$ is an endemic equilibrium of system (1.1). □

Remark 3.7 Note that if two patches are isolated and double exposures do not influence the infection rate (i.e., $\nu_i = 0$), then the disease spreads in the ith patch if $R_{0i} > 1$ and goes extinct if $R_{0i} < 1$ (see (2.9) and Table 1). If individuals disperse between two patches, and all travel rates for susceptible, infective and recovered individuals are positive constants and equal (i.e., $\theta_{ij}^S = \theta_{ij}^R = 0$, $M_{ij}^S = M_{ij}^R = b_{ij} > 0$, $i, j = 1, 2$, $i \ne j$) and $\nu_i = 0$, $i = 1, 2$ in system (1.1), we still have a threshold dynamic result (see Theorems 3.5 and 3.6):

(a) The disease will die out for all positive initial populations if $R_0 < 1$;
(b) The disease will persist for all positive initial populations if $R_0 > 1$.

3.2 Numerical simulations when $\nu_1 = \nu_2 = 0$

In the following numerical simulations, we choose the travel rates as Type I in (1.4) if they depend on the disease prevalence. When $\nu_1 = \nu_2 = 0$, the incidence rate in system (1.1) is bilinear incidence: $\lambda_i(I_i) I_i S_i = \beta_i I_i S_i$, under which the isolated patch model (2.2) admits simple threshold dynamics.

In this subsection, to investigate the effect of population dispersal on disease spread, we always assume $\nu_1 = \nu_2 = 0$, initial values: $N_1(0) = 1 \times 10^6$, $N_2(0) = 1 \times 10^5$, $I_1(0) = 1 \times 10^5$, $I_2(0) = 1 \times 10^4$, $R_1(0) = R_2(0) = 1$, and $b_1, b_2, d_1, d_2, \alpha_1, \alpha_2, \gamma_1, \gamma_2$ are given in Table 2.

3.2.1 Travel rates are independent of disease status and disease prevalence

We next present two examples with conditions satisfying Remark 3.7, i.e., $\theta_{ij}^S = \theta_{ij}^R = 0$, $M_{ij}^S = M_{ij}^R = b_{ij}$ $(i, j = 1, 2, i \ne j)$, to investigate the relationship between R_0

Table 3 Parameters of system (1.1)

Case	β_1	β_2	R_{01}	R_{02}
(1)	7×10^{-7}	5×10^{-6}	0.8739	0.996
(2)	9×10^{-7}	5×10^{-6}	1.1236	0.996

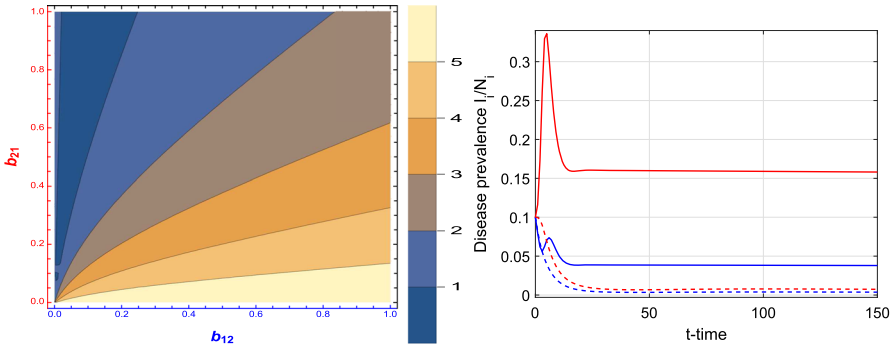

Fig. 3 **a** Contour plot of R_0 versus b_{12} and b_{21} when $R_{01} < R_{02} < 1$. **b** Disease prevalence: $\frac{I_1}{N_1}$ (blue), $\frac{I_2}{N_2}$ (red). $(b_{12}, b_{21}) = (0.2, 0.2)$ (solid curves); $(b_{12}, b_{21}) = (0.2, 0.9)$ (dashed curves). The other parameters are given in Table 2 and Table 3(1) (color figure online)

and R_{0i} and how R_0 changes with the travel rates b_{12} and b_{21}. Choosing β_1 and β_2 as listed in Table 3. In all two scenarios, patch 2 has higher transmission rates, i.e., $\beta_2 > \beta_1$ (Figs. 3 and 4).

Example 1 Case (1) in Table 3: $R_{01} < R_{02} < 1$. In this case, the disease dies out in each isolated patch. The contour plot of R_0 versus b_{12} and b_{21} is given in Fig. 3a, which shows that an increase in b_{21} will decrease R_0. Conversely, for fixed b_{21}, an increase in b_{12} will increase R_0. Consequently, although the disease dies out in each isolated patch, increasing travel rates from patch 1 (low-risk) to patch 2 (high-risk) may cause the disease to become endemic in both patches, i.e., the inappropriate population travel may intensify the disease spread.

For example, fix $b_{12} = b_{21} = 0.2$, then $R_0 \approx 3.0321$, i.e., the disease spreads in both patches (solid curves in Fig. 3b), thus travel intensifies the spread of disease, turning originally low-risk patchs into high-risk patchs. For $b_{12} = 0.2$, $b_{21} = 0.9$, $R_0 \approx 0.9685$, i.e., the disease disappears in both patches (dashed curves in Fig. 3b), thus travel reduces the spread of disease, turning originally high-risk patches into low-risk patches. The disease prevalence is higher in patch 2 (high-risk and higher infection rate) when $b_{12} = b_{21}$.

Example 2 Case (2) in Table 3: $R_{01} > 1$, $R_{02} < 1$. The disease will persist in isolated patch 1 and disappear in isolated patch 2. The contour plot of R_0 versus b_{12} and b_{21} is shown in Fig. 4a, which shows the similar results as *Example* 1 when population dispersal occurs. For example, for fixed $b_{21} = 0.1$, we have $R_0 \approx 3.3764$ if $b_{12} = 0.1$ (solid curves in Fig. 4b); $R_0 \approx 4.4706$ if $b_{12} = 0.3$ (dashed curves in Fig. 4b);

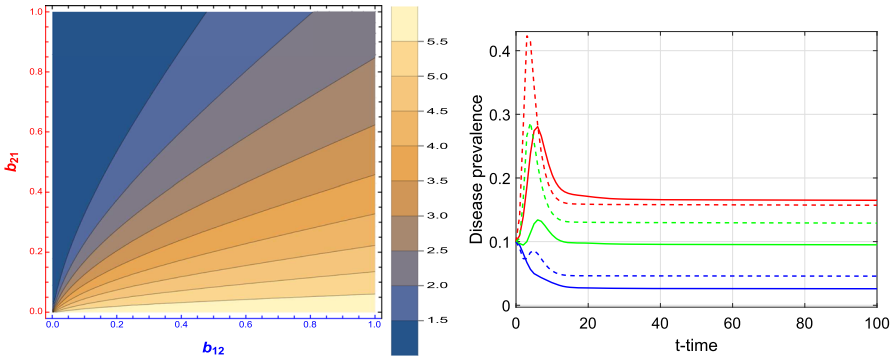

Fig. 4 **a** Contour plot of R_0 versus b_{12} and b_{21} when $R_{01} > 1$ and $R_{02} < 1$. **b** Disease prevalence: $\frac{I_1}{N_1}$ (blue), $\frac{I_2}{N_2}$ (red), $\frac{I_1+I_2}{N_1+N_2}$ (green). $(b_{12}, b_{21}) = (0.1, 0.1)$ (solid curves); $(b_{12}, b_{21}) = (0.3, 0.1)$ (dashed curves) (color figure online)

thus travel intensifies the spread of disease, turning originally low-risk patches into high-risk patches. Moreover, increasing the travel from patch 1 (high-risk) to patch 2 (low-risk) will increase R_0 and the overall disease prevalence. For fixed $b_{21} = 0.1$ and bigger b_{12}, the disease prevalence of patch 1 and both patches become higher, while higher first and then lower for patch 2, moreover, the disease outbreaks earlier. The disease prevalence is higher in patch 2 (low-risk) when $b_{12} = b_{21}$ since $\beta_2 > \beta_1$.

Remark 3.8 When β_2 is much larger than β_1 and R_{01} is little difference from R_{02}, Figs. 3**a** and 4a imply that R_0 is monotonic, i.e., R_0 decreases as b_{21} increases for fixed b_{12}; R_0 increases as b_{12} increases for fixed b_{21}. While R_0 may be nonmonotonic when R_{01} is much larger than R_{02} and β_1 is a bit smaller than β_2, for example, when b_{12} is fixed, Fig. 5 shows that R_0 may decrease first and then increase as b_{21} increases, which indicates that, although patch 1 has a lower infection rate ($\beta_1 < \beta_2$), increasing travel from patch 2 to patch 1 may cause disease more serious when R_{01} is much larger than R_{02}. Therefore, so as to control a disease, it is necessary to control reasonably the travel rates by considering the joint effect of the infection rate (β_i) and the risk of disease outbreak (R_{0i}) of each patch.

Remark 3.9 The above analyses indicate that the reproduction number R_0 of system (1.1) can be greater than the reproduction number R_{0i} of each isolated patch, i.e., $R_0 \leq \max_{1\leq i\leq n} \{R_{0i}\}$ does not hold, which violates the known results when the disease is standard incidence (Wang and Mulone 2003; Salmani and van den Driessche 2006).

3.2.2 Infectives do not travel

If the parameters do not satisfy the conditions in Remark 3.7, then R_0 may not be a threshold between disease extinction and persistence. We next present some numerical

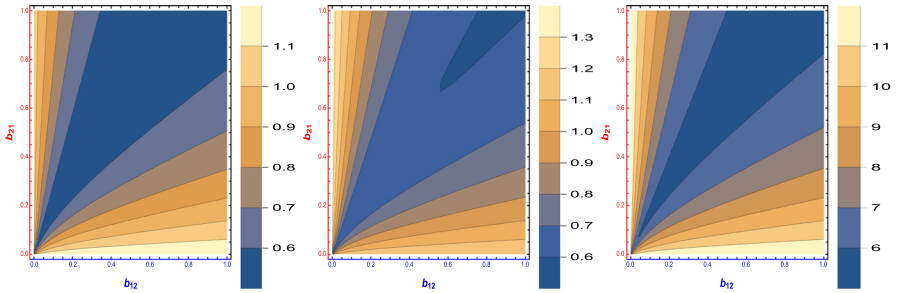

Fig. 5 Contour plots of R_0 versus b_{12} and b_{21} with different $\beta_1,\ \beta_2$. **a** $R_{01} \approx 0.8739,\ R_{02} \approx 0.1992$ with $\beta_1 = 7 \times 10^{-7},\ \beta_2 = 1 \times 10^{-6}$; **b** $R_{01} \approx 1.1236,\ R_{02} \approx 0.1992$ with $\beta_1 = 9 \times 10^{-7},\ \beta_2 = 1 \times 10^{-6}$; **c** $R_{01} \approx 9.9875,\ R_{02} \approx 1.992$ with $\beta_1 = 8 \times 10^{-6},\ \beta_2 = 1 \times 10^{-5}$

simulations to investigate the dependence of disease spread on the dispersal rates of susceptible and recovered individuals when infective individuals of both patches do not travel. Some parameters in system (1.1) are taken from Table 2.

Unidirectional and constant dispersal firstly, when the travel of infective and recovered individuals is prohibited and the travel rates of susceptible individuals do not depend on the relative severity of the disease in two patches, we explore the impact of the travel of susceptible individuals on disease spread (Fig. 6).

Let β_1 and β_2 take the values in Case (2) of Table 3 ($R_{01} > 1,\ R_{02} < 1$), then the disease persists in isolated patch 1 and disappears in isolated patch 2. Figure 6a shows that the travel of susceptible individuals from patch 2 to patch 1 increases the disease prevalence of patch 1 (the blue dashed curve) and the overall disease prevalence (the green dashed curve in Fig. 6d), and the disease in patch 2 still disappears (the red dashed curve). However, Fig. 6b shows that the travel of susceptible individuals from patch 1 to patch 2 makes the disease in patch 2 become endemic (the red dashed curve), the disease in patch 1 disappears (the blue dashed curve), and the overall disease prevalence increases (Fig. 6e). As the travel rate of susceptible individuals from patch 1 to patch 2 increases, Fig. 6c shows that the disease prevalence of patch 2 increases (the red dashed curve) and the disease outbreaks earlier in patch 2, the disease in patch 1 disappears (blue dashed curves), and the overall disease prevalence increases (Fig. 6f).

Hence, the results here indicate that the unidirectional and constant dispersal of susceptible individuals will make the disease more serious. Moreover, the travel of susceptible individuals from patch 1 to patch 2 will markedly aggravate the overall disease prevalence.

Relative prevalence-based dispersal secondly, we explore the effect of relative prevalence-based dispersal for susceptible and recovered individuals on disease transmission. Let $b_{12} = b_{21} = 0$ (i.e., the travel of infective individuals is prohibited), $(\beta_1,\ \beta_2)$ takes the values in Case (1) of Table 3 ($R_{01} < R_{02} < 1$), and the solid (resp. dashed) curves represent $\theta_{12}^S = \theta_{21}^S = \theta_{12}^R = \theta_{21}^R = 0$ (resp. $\theta_{12}^S = \theta_{21}^S = 1$,

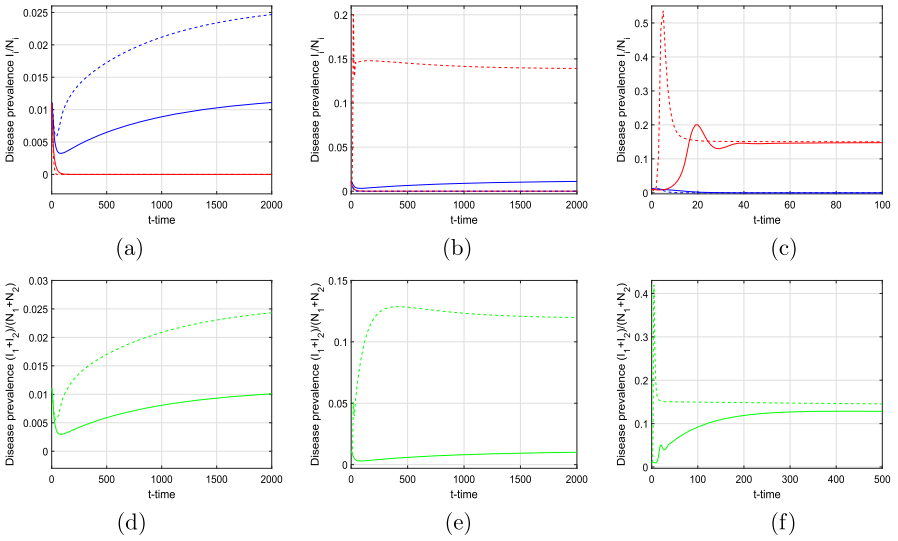

Fig. 6 Disease prevalence when $\theta_{ij}^S = b_{ij} = M_{ij}^R = 0$ $(i, j = 1, 2, i \neq j)$: $\frac{I_1}{N_1}$ (blue), $\frac{I_2}{N_2}$ (red), $\frac{I_1+I_2}{N_1+N_2}$ (green). β_i takes Case (2) in Table 3. **a**, **d** $(M_{12}^S, M_{21}^S) = (0, 0)$ (solid curves), $(M_{12}^S, M_{21}^S) = (0, 0.01)$ (dashed curves). **b**, **e** $(M_{12}^S, M_{21}^S) = (0, 0)$ (solid curves), $(M_{12}^S, M_{21}^S) = (0.01, 0)$ (dashed curves). **c**, **f** $(M_{12}^S, M_{21}^S) = (0.01, 0)$ (solid curves), $(M_{12}^S, M_{21}^S) = (0.1, 0)$ (dashed curves) (color figure online)

Table 4 Parameter values of system (1.1) with $\theta_{ij}^S = \theta_{ij}^R = 0$, $M_{ij}^S = M_{ij}^R = 0.3$

Case	(1)	(2)	(3)	(4)	(5)	(6)
b_{12}	0	0	0.01	0.1	0	0.1
b_{21}	0	0.01	0	0.1	0.1	0

$\theta_{12}^R = \theta_{21}^R = 0.1$). Figure 7 implies that the disease persists in patch 2 and disappears in patch 1 (solid curves) if the travel rates of susceptible and recovered individuals do not depend on the relative severity of the disease in two patches. If the travel rates depend on the relative severity of the disease in two patches, then the disease prevalence of patch 2 decreases (red dashed curves compared with red solid curves in Fig. 7), the disease still disappears in patch 1, the overall disease prevalence will decrease (green curves in Fig. 7).

Therefore, the relative prevalence-based dispersal for susceptible and recovered individuals may reduce the overall prevalence of the disease.

3.2.3 Infective individuals travel

We next explore the impact of the travel of infective individuals on the disease spread when the travel rates of susceptible and recovered individuals are fixed constants.

Let (β_1, β_2) takes the values in Case (1) in Table 3 ($R_{01} < R_{02} < 1$), $\theta_{ij}^S = \theta_{ij}^R = 0$, $M_{ij}^S = M_{ij}^R = 0.3$. Then the disease persists in patch 2 (the red solid curve in Fig. 8a) and disappears in patch 1 (the blue solid curve in Fig. 8a) if $b_{12} = b_{21} = 0$.

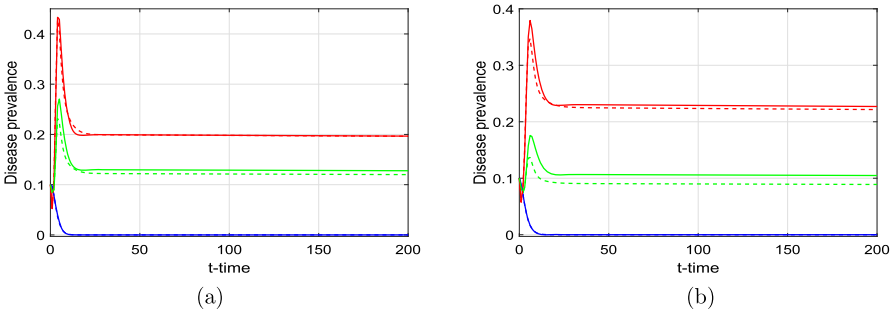

Fig. 7 Disease prevalence when $b_{ij} = 0$ $(i, j = 1, 2, i \neq j)$: $\frac{I_1}{N_1}$ (blue), $\frac{I_2}{N_2}$ (red), $\frac{I_1+I_2}{N_1+N_2}$ (green). $\theta_{12}^S = \theta_{21}^S = \theta_{12}^R = \theta_{21}^R = 0$ (solid curves), $\theta_{12}^S = \theta_{21}^S = 1$, $\theta_{12}^R = \theta_{21}^R = 0.1$ (dashed curves). **a** $(M_{12}^S, M_{21}^S, M_{12}^R, M_{21}^R) = (0.3, 0.2, 0.3, 0.2)$; **b** $(M_{12}^S, M_{21}^S, M_{12}^R, M_{21}^R) = (0.2, 0.3, 0.2, 0.3)$ (color figure online)

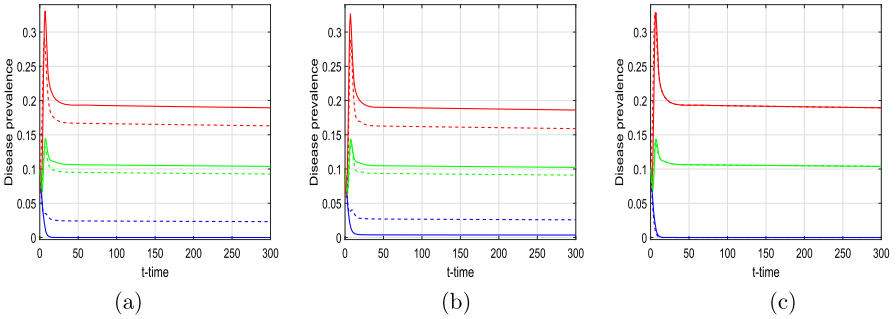

Fig. 8 Disease prevalence when infective individuals travel: $\frac{I_1}{N_1}$ (blue), $\frac{I_2}{N_2}$ (red), $\frac{I_1+I_2}{N_1+N_2}$ (green). (b_{12}, b_{21}) in Table 4 takes: **a** case (1) (solid curves), case (4) (dashed curves). **b** case (2) (solid curves), case (5) (dashed curves). **c** case (3) (solid curves), case (6) (dashed curves) (color figure online)

Figure 8a shows that the disease become endemic in both patches (dashed curves) if $b_{12} = b_{21} = 0.1$, where the disease prevalence of patch 2 decreases (the red dashed curve), the disease prevalence of patch 1 increases (the blue dashed curve), and the overall disease prevalence decreases (the green dashed curve). Figure 8b shows that the overall disease prevalence decreases as the travel rate of infective individuals from patch 2 to patch 1 increases. However, Fig. 8c shows that the disease will not be affected as the travel rate of infective individuals from patch 1 to patch 2 increases.

Hence, the results here indicate that the reasonable travel of infective individuals may reduce the overall disease prevalence because medical resources can be fully utilized. In order to make full use of medical resources, transferring infective individuals to places with more affluent medical care under the condition of ensuring full isolation of infective individuals can reduce the total prevalence of diseases.

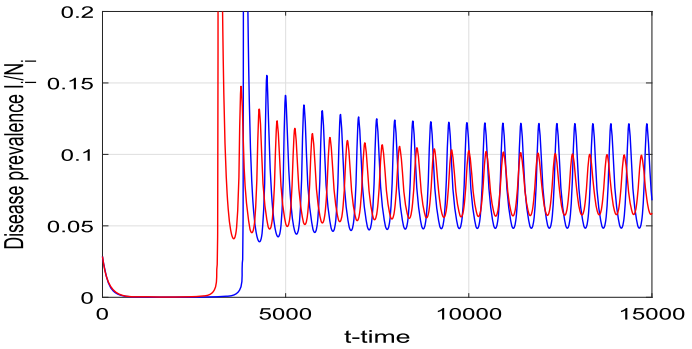

Fig. 9 Disease prevalence in model (1.1) with no travel and $\nu_1\nu_2 \neq 0$: $\frac{I_1}{N_1}$ (blue), $\frac{I_2}{N_2}$ (red). Where $b_1 = b_2 = 10680$, $d_1 = d_2 = 0.001$, $\alpha_1 = \alpha_2 = 0.01479$, $\gamma_1 = \gamma_2 = 0.0003441$, $\nu_1 = \nu_2 = 0.00001$, $\beta_1 = 1.68 \times 10^{-9}$ and $\beta_2 = 1.72 \times 10^{-9}$ (color figure online)

3.3 Numerical simulations when $\nu_1\nu_2 \neq 0$

When $\nu_1\nu_2 \neq 0$, the incidence rate in model (1.1) is nonlinear: $\lambda_i(I_i)I_iS_i = \beta_i(1 + \nu_i I_i)I_iS_i$. In the following numerical simulations, we choose the travel rates as Type I in (1.4) if they depend on the disease prevalence.

In Sect. 2, we have shown complex dynamics and bifurcations in model (2.2) [i.e., single patch model (1.5)], such as the existence of a stable limit cycle encircling a unique positive equilibrium E_+ in Fig. 2a, where $(R_{0i}, p, A, q) \in \Gamma_{11} \times \Lambda$ and $R_{0i} = \frac{133}{117} > 1$, i.e., the disease persists in the form of a stable periodic outbreak in each isolated patch for almost all positive initial values. We next explore the effect of population dispersal on the disease spread in patch model (1.1).

we always assume initial values: $N_1(0) = N_2(0) = 3.5 \times 10^6$, $I_1(0) = I_2(0) = 1 \times 10^5$, $R_1(0) = R_2(0) = 1$, and fix the parameters in each isolated patch as those in Fig. 2a except for a slight larger β_2 in patch 2. When no travel occurs in model (1.1), disease prevalence of patch 1 and patch 2 are shown in Fig. 9, where disease prevalence of each isolated patch exhibits regular periodic oscillations.

Unidirectional and constant dispersal firstly, we explore the impact of the unidirectional and constant travel of susceptible or infective individuals on disease spread (Figs. 10 and 11).

Figure 10 shows the effect of the travel of susceptible individuals from patch 2 to patch 1. In Fig. 10a, the periodic outbreak of the disease in patch 2 is delayed and the oscillation amplitude becomes larger; the disease in patch 1 first tends to a positive steady state, and then complex periodic patterns like mixed-mode oscillations (MMOs). As the travel from patch 2 to patch 1 increases, in Fig. 10b, the disease dies out in patch 2 while tends to a positive steady state in patch 1.

Figure 11 shows the effect of infective individuals travel between two patches. Figure 11a shows that $\frac{I_1}{N_1}$ first tends a small-amplitude periodic oscillation and then complex MMOs, while $\frac{I_2}{N_2}$ first tends to zero and then a large-amplitude relaxation oscillation (or 1-1 mode MMOs). When b_{21} increases, Fig. 11b shows that $\frac{I_1}{N_1}$ tends a

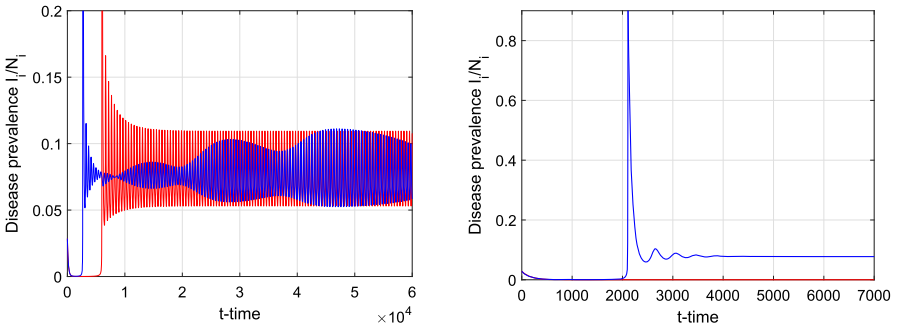

Fig. 10 Infection proportions when susceptible individuals travel and $\theta_{ij}^S = M_{ij}^R = b_{ij} = 0$ $(i, j = 1, 2, i \neq j)$: $\frac{I_1}{N_1}$ (blue), $\frac{I_2}{N_2}$ (red). **a** $M_{12}^S = 0$, $M_{21}^S = 0.0001$. **b** $M_{12}^S = 0$, $M_{21}^S = 0.0002$ (color figure online)

regular periodic oscillation and $\frac{I_2}{N_2}$ tends to zero. Figure 11c and d show similar results as Fig. 11a and b, respectively.

The results here indicate that small unidirectional and constant dispersal rates can lead to complex periodic patterns like large-amplitude relaxation oscillations or small-amplitude Mixed-mode oscillations (MMOs), whereas large unidirectional and constant dispersal rates can make the disease go extinct in one patch and persist in the form of a positive steady state or a periodic solution in the other patch.

Unidirectional and relative prevalence-based dispersal secondly, we explore the effect of relative prevalence-based dispersal for susceptible and recovered individuals on disease transmission.

Figure 12 shows unidirectional movement from patch 2 to patch 1. Figure 12a shows that $\frac{I_1}{N_1}$ first tends to a positive steady state and then a regular periodic oscillation with smaller amplitude, $\frac{I_2}{N_2}$ first tends to zero and then a regular periodic oscillation with larger amplitude, $\frac{I_1}{N_1}$ and $\frac{I_2}{N_2}$ tend to periodic patterns much later (compared with Fig. 9). Figure 12a–b shows that $\frac{I_1}{N_1}$ and $\frac{I_2}{N_2}$ tend to regular periodic patterns earlier if susceptible and recovered individuals depend on the relative severity of the disease.

The results here indicate that unidirectional and relative prevalence-based dispersal rates for susceptible and recovered individuals can make periodic outbreak earlier.

4 Discussion

In this paper, we proposed an SIRS patch model with a nonlinear incidence rate and relative prevalence-based dispersal rates, where the dispersal rates of susceptible and recovered individuals depend on the relative severity of the disease in two patches.

In an isolated environment, model (1.1) becomes as model (1.5) with a nonlinear incidence rate (1.2), which has been studied by van den Driessche and Watmough

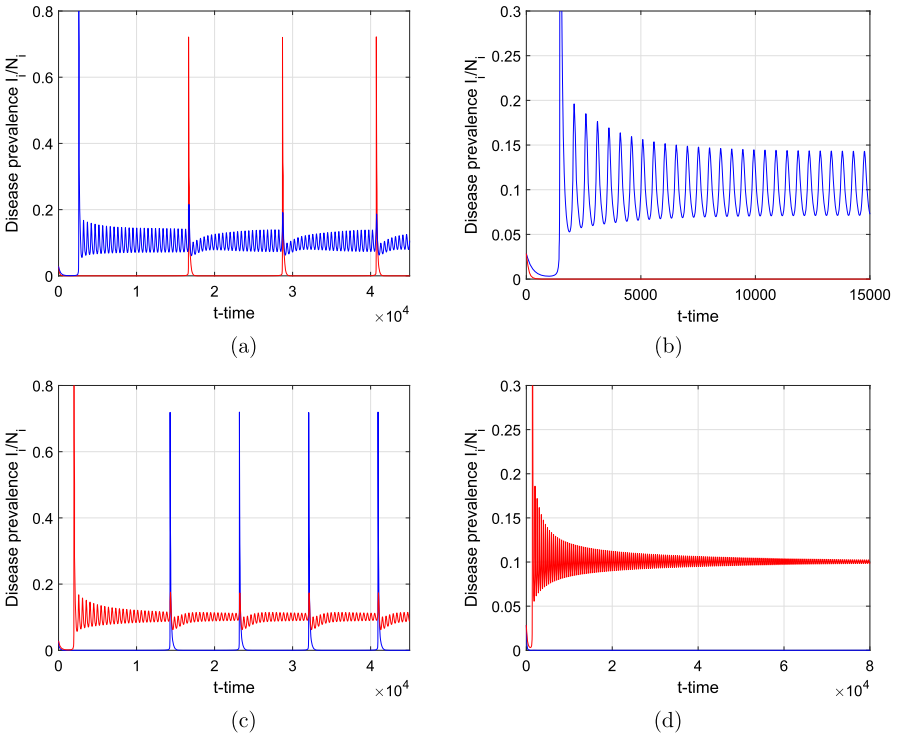

Fig. 11 Disease prevalence when infective individuals travel and $\theta_{ij}^S = \theta_{ij}^R = 0$, $M_{ij}^S = 0.0001$, $M_{ij}^R = 0.001$ $(i, j = 1, 2, i \neq j)$: $\frac{I_1}{N_1}$ (blue), $\frac{I_2}{N_2}$ (red). **a** $b_{12} = 0$, $b_{21} = 0.002$. **b** $b_{12} = 0$, $b_{21} = 0.003$. **c** $b_{12} = 0.0015$, $b_{21} = 0$. **d** $b_{12} = 0.002$, $b_{21} = 0$ (color figure online)

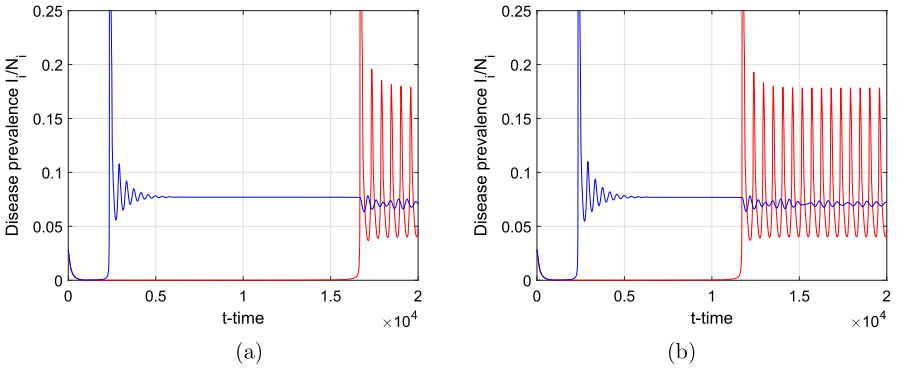

Fig. 12 Infection proportions when $M_{12}^S = M_{12}^R = 0$, $b_{ij} = 0$ $(i, j = 1, 2, i \neq j)$: $\frac{I_1}{N_1}$ (blue), $\frac{I_2}{N_2}$ (red). **a** $M_{21}^S = M_{21}^R = 0.00015$, $\theta_{21}^S = \theta_{21}^R = 0$; **b** $M_{21}^S = M_{21}^R = 0.00015$, $\theta_{21}^S = 1$, $\theta_{21}^R = 0.1$ (color figure online)

(2003) and Jin et al. (2007). While the complete bifurcation phenomena still remain unclear, especially for the degenerate Bogdanov–Takens and Hopf bifurcations. In this paper, we have shown the existence of a nilpotent cusp of codimension up to 3, around which model (1.5) can undergo degenerate Bogdanov–Takens bifurcation of codimension 3 and no bifurcations with higher codimension. Moreover, when model (1.5) admits a center-type equilibrium, we have shown that it is a weak focus with order up to 2, around which model (1.5) can exhibit Hopf bifurcation with codimension up to 2. Our results indicate the nonlinear incidence rate can determine the transmission dynamics of epidemics. More precisely, there exists two critical values β^*, β_* ($\beta^* < \beta_*$) for infection rate β_i (due to single contact) and two critical values $\frac{d_i}{b_i}$, ν_* $\left(\frac{d_i}{b_i} < \nu_*\right)$ for infection rate ν_i (due to double exposures), such that: **(i)** when $\beta_i < \beta^*$, the disease will die out for all positive initial densities; **(ii)** when $\beta^* < \beta_i < \beta_*$, the disease will die out for all positive initial densities if $\nu_i < \nu_*$; the disease may die out for some positive initial densities, and persist in the form of coexistent periodic oscillations or coexistent steady states for other positive initial densities if $\nu_i > \nu_*$; **(iii)** when $\beta_i > \beta_*$, the disease will persist in the form of a unique coexistent steady state for all positive initial densities if $\nu_i \leq \frac{d_i}{b_i}$; the disease may persist in the form of a unique coexistent steady state or periodic coexistent oscillations for all positive initial densities if $\nu_i > \frac{d_i}{b_i}$. Moreover, our results indicate the importance of the rate ν_i of new infective individuals arising from double exposures: **(i)** when $\nu_i < \nu_*$, whether the disease persists or dies out will depend on the relative size of β_i and β_*. If we can control the infection rate β_i such that $\beta_i < \beta_*$, then the disease will disappear; **(ii)** when $\nu_i > \nu_*$, system (1.5) may exhibit backward bifurcation with rich dynamics. To make the disease disappear, we need to further control the infection rate β_i such that $\beta_i < \beta^*$.

In a connected environment, we first calculated the basic reproduction number R_0 for model (1.1), and then showed that the global attractivity of the disease-free equilibrium can be preserved if $R_0 < 1$, $\nu_i = 0$ ($i = 1, 2$) and the dispersal rates of all individuals are identical constants. When $R_0 > 1$ and $b_{ij} > 0$ ($i, j = 1, 2, i \neq j$) (dispersal rates of infective individuals), system (1.1) admits at least one endemic equilibrium and the disease is uniformly persistent. Therefore, we establish a threshold between the extinction and the uniform persistence of the disease under some restricted conditions.

Secondly, by numerical simulations, we explored the effect of populations dispersal on disease transmission under the assumptions: $\nu_i = 0$ (bilinear incidence), patch 1 has a lower infection rate than patch 2. We have the following results:

(1) Travel rates are independent of disease status and disease prevalence:

   (i) R_0 may be nonmonotonic w.r.t. dispersal rates when R_{01} is much larger than R_{02} and β_1 is a bit smaller than β_2;
   (ii) $R_0 \leq \max\{R_{01}, R_{02}\}$ does not hold for some cases.

(2) Infective individuals of both patches do not travel:

   (i) The unidirectional and constant dispersal of susceptible individuals will make the disease more serious. Moreover, the travel of susceptible individuals from patch 1 to patch 2 will markedly aggravate the overall disease prevalence;

(ii) The relative prevalence-based dispersal for susceptible and recovered individuals may reduce the overall prevalence of the disease.

(3) Travel of infective individuals from patch 2 to patch 1 can reduce the overall disease prevalence because medical resources can be fully utilized.

Thirdly, when the disease persists in the form of a stable periodic outbreak in each isolated patch, we explored the effect of populations dispersal under the assumptions: $\nu_i \neq 0$ (nonlinear incidence), two patches have identical demography and a slight lower infection rate for patch 1. We have the following results:

(1) Small unidirectional and constant dispersal rates can lead to complex periodic patterns like large-amplitude relaxation oscillations or small-amplitude Mixed-mode oscillations (MMOs);
(2) large unidirectional and constant dispersal rates can make the disease go extinct in one patch and persist in the form of a positive steady state or a periodic solution in the other patch;
(3) Unidirectional and relative prevalence-based dispersal rates for susceptible and recovered individuals can make periodic outbreak earlier.

Therefore, in order to control the spread of diseases, we need to control reasonably not only the travel of infective individuals, but also the travel of susceptible and recovered individuals, by considering the joint effect of the population structure, infection rate and disease outbreak risk of each patch. And, in order to make full use of medical resources, transferring infective individuals to places with more affluent medical care under the condition of ensuring full isolation of infective individuals can reduce the total prevalence of diseases to a certain extent. Moreover, small, unidirectional and constant dispersal rates can induce large-amplitude relaxation oscillations, which imply a larger periodic outbreak of the disease, or induce Mixed-mode oscillations where small- and large-amplitude oscillations alternate (Fig. 11).

There are some unanswered questions. For system (2.1): In region $\Gamma_{11} \times \Lambda$, is the unique positive equilibrium E_+ global asymptotic stability when it is locally asymptotically stable? Does there exist a unique limit cycle when the unique positive equilibrium E_+ is unstable? Whether the maximum number of limit cycles is 2 in system (2.1)? For system (1.1): If $R_0 < 1$, $\nu_i = 0$ and dispersal rates of all populations are different, whether the disease free equilibrium E^0 is still globally attractive. If $R_0 > 1$ and $\nu_i = 0$, whether the endemic equilibrium is unique and globally attractive? What if $\nu_i > 0$?

Declarations

Conflict of Interests The authors have no competing interests to declare that are relevant to the content of this article.

References

Alexander ME, Moghadas SM (2004) Periodicity in an epidemic model with a generalized non-linear incidence. Math Biosci 189:75–96

Allen LJS, Bolker BM, Lou Y, Nevai AL (2007) Asymptotical profiles of the steady states for an SIS epidemic patch model. SIAM J Appl Math 67:1283–1309
Arino J, Ducrot A, Zongo P (2012) A metapopulation model for malaria with transmission-blocking partial immunity in hosts. J Math Biol 64:423–448
Arsie A, Kottegoda C, Shan C (2022) A predator-prey system with generalized Holling type IV functional response and Allee effects in prey. J Differ Equ 309:704–740
Chinazzi M, Davis JT, Ajelli M et al (2020) The effect of travel restrictions on the spread of the (2019) novel coronavirus (COVID-19) outbreak. Science 368:395–400
Chow S-N, Li C, Wang D (1994) Normal forms and bifurcations of Plannar vector fields. Cambridge University Press, Chicago
Cosner C, Beier JC, Cantrell RS, Impoinvil D, Kapitanski L, Potts MD, Troyo A, Ruan S (2009) The effects of human movement on the persistence of vector-borne diseases. J Theor Biol 258:550–560
Dumortier F, Roussarie R, Sotomayor J (1987) Generic 3-parameter families of vector fields on the plane, unfolding a singularity with nilpotent linear part. The cusp case of codimension 3. Ergod Theor Dyn Syst 7(3):375–413
Diekmann O, Heesterbeek JAP, Roberts MG (2010) The construction of next-generation matrices for compartmental epidemic models. J R Soc Interface 7:873–885
Gao D (2020) How does dispersal affect the infection size? SIAM J Appl Math 80:2144–2169
Gao D, Ruan S (2012) A multipatch malaria model with logistic growth populations. SIAM J Appl Math 72:819–841
Gao D, Cosner C, Cantrell RS, Beier JC, Ruan S (2013) Modeling the spatial spread of Rift Valley fever in Egypt. Bull Math Biol 75:523–542
Gao D, Lou Y (2021) Impact of state-dependent dispersal on disease prevalence. J Nonlinear Sci 31(5):1–41
Hsieh Y-H, van den Driessche P, Wang L (2007) Impact of travel between patches for spatial spread of disease. Bull Math Biol 69:1355–1375
Hotle S, Mumbower S (2021) The impact of COVID-19 on domestic U.S. air travel operations and commercial airport service. Transp Res Interdiscip Perspect 9:100277
International Organization for Migration, COVID-19 Travel Restrictions Output (2020) https://migration.iom.int/reports/covid-19-travel-restrictions-output-%E2%80%94-12-october-2020
Jin Y, Wang W (2005) The effect of population dispersal on the spread of a disease. J Math Anal Appl 308:343–364
Jin Y, Wang W, Xiao S (2007) An SIRS model with a nonlinear incidence rate, Chaos Solit. Fractals 34:1482–1497
Li J, Zhou Y, Wu J, Ma Z (2007) Complex dynamics of a simple epidemic model with a nonlinear incidence. Discrete Contin Dyn Syst Ser B 8:161–173
Li C, Li J, Ma Z, Zhu H (2014) Canard phenomenon for an SIS epidemic model with nonlinear incidence. J Math Anal Appl 420:987–1004
Li C, Li J, Ma Z (2015) Codimension 3 B-T bifurcations in an epidemic model with a nonlinear incidence. Discrete Contin Dyn Syst Ser B 20:1107–1116
Lu M, Huang J, Ruan S, Yu P (2019) Bifurcation analysis of an SIRS epidemic model with a generalized nonmonotone and saturated incidence rate. J Differ Equ 267:1859–1898
Lu M, Huang J, Ruan S, Yu P (2021) Global dynamics of a susceptible-infectious-recovered epidemic model with a generalized nonmonotone incidence rate. J Dyn Differ Equ 33(4):1625–1661
Lu M, Huang J, Wang H (2023) An organizing center of codimension four in a predator–prey model with generalist predator: from tristability and quadristability to transients in a nonlinear environmental change. SIAM J Appl Dyn Syst (in press)
Pan Q, Huang J, Wang H (2022) An SIRS model with nonmonotone incidence and saturated treatment in a changing environment. J Math Biol 85:23
Salmani M, van den Driessche P (2006) A model for disease transmission in a patchy environment. Discrete Contin Dyn Syst Ser B 6:185–202
The World Bank Group (2022a) Air transport, passengers carried https://data.worldbank.org/indicator/IS.AIR.PSGR
The World Bank Group (2022b) Urban population (% of total population) https://data.worldbank.org/indicator/SP.URB.TOTL.IN.ZS
Thieme HR (1993) Persistence under relaxed point-dissipativity (with application to an endemic model). SIAM J Math Anal 24:407–435

van den Driessche P, Watmough J (2000) A simple SIS epidemic model with a backward bifurcation. J Math Biol 40:525–540
van den Driessche P, Watmough J (2002) Reproduction numbers and sub-threshold endemic equilibria for compartmental models of disease transmission. Math Biosci 180:29–48
van den Driessche P, Watmough J (2003) Epidemic solutions and endemic catastrophes. Fields Inst Commun 36:247–257
Wang W, Mulone G (2003) Threshold of disease transmission in a patch environment. J. Math. Anal. Appl. 285:321–335
Wang H, Salmaniw Y (2023) Open problems in PDE models for cognitive animal movement via nonlocal perception and mental mapping (under review)
Wang W, Zhao X-Q (2004) An epidemic model in a patchy environment. Math. Biosci. 190:97–112
Wang H, Wang K, Kim YJ (2022) Spatial segregation in reaction-diffusion epidemic models. SIAM J. Appl. Math. 82:1680–1709
Wu JT, Leung K, Leung GM (2020) Nowcasting and forecasting the potential domestic and international spread of the 2019-nCoV outbreak originating in Wuhan, China: A modelling study. Lancet 395:689–697
Xiang C, Huang J, Ruan S, Xiao D (2019) Bifurcation analysis in a host-generalist parasitoid model with Holling II functional response. J. Differential Equations 268(8):4618–4662
Xue L, Jing S, Zhang K, Milne R, Wang H (2022) Infectivity versus fatality of SARS-CoV-2 mutations and influenza. Int. J. Infect. Dis. 121:195–202
Yang W, Sun C, Arino J (2020) Effect of media-induced modification of travel rates on disease transmission in a multiple patch setting. J. Appl. Anal. Comput. 10:2682–2703
Zhang Z, Ding T, Huang W, Dong Z (1992) Qualitative theory of differential equations, Translations of Mathematical Monographs, vol 101. American Mathematical Society, Providence, RI
Zhang H, Niu B, Wang H (2023a) Formulation and analysis of multi-patch models under memory-based dispersal (under review)
Zhang H, Wang H, Wei J (2023b) Perceptive movement of susceptible individuals with memory (under review)
Zhao X-Q (1995) Uniform persistence and periodic coexistence states in infinite dimensional periodic semiflows with applications. Can. Appl. Math. Quart. 3:473–495
Zhao X-Q (2003) Dynamical systems in population biology. Springer, Berlin

Authors and Affiliations

Min Lu[1] · Daozhou Gao[2,3] · Jicai Huang[1] · Hao Wang[4]

Min Lu
lumin@mails.ccnu.edu.cn

Daozhou Gao
d.gao51@csuohio.edu

[1] School of Mathematics and Statistics and Hubei Key Laboratory of Mathematical Sciences, Central China Normal University, Wuhan 430079, Hubei, People's Republic of China

[2] Present Address: Department of Mathematics, Cleveland State University, Cleveland 44115, Ohio, USA

[3] Department of Mathematics, Shanghai Normal University, Shanghai 200234, People's Republic of China

[4] Department of Mathematical and Statistical Sciences, University of Alberta, Edmonton T6G 2G1, AB, Canada